Cajal-Retzius neurons are required for the development of the human hippocampal fissure

Gundela Meyer,[1] Emilio González-Arnay,[2] Ute Moll,[3] Alice Nemajerova,[3] Fadel Tissir[4] and Miriam González-Gómez[1]

[1]Department of Basic Medical Sciences, University La Laguna, La Laguna, Spain
[2]Department of Anatomy and Neuroscience, Autonomous University Madrid, Madrid, Spain
[3]Department of Pathology, Stony Brook University, Stony Brook, NY, USA
[4]Developmental Neurobiology Group, Institute of NeuroScience, UCL Louvain, Brussels, Belgium

Abstract

Cajal-Retzius neurons (CRN) are the main source of Reelin in the marginal zone of the developing neocortex and hippocampus (HC). They also express the transcription factor p73 and are complemented by later-appearing GABAergic Reelin+ interneurons. The human dorsal HC forms at gestational week 10 (GW10), when it develops a rudimentary Ammonic plate and incipient dentate migration, although the dorsal hippocampal fissure (HF) remains shallow and contains few CRN. The dorsal HC transforms into the indusium griseum (IG), concurrently with the rostro-caudal appearance of the corpus callosum, by GW14–17. Dorsal and ventral HC merge at the site of the former caudal hem, which is located at the level of the future atrium of the lateral ventricle and closely connected with the choroid plexus. The ventral HC forms at GW11 in the temporal lobe. The ventral HF is wide open at GW14–16 and densely populated by large numbers of CRNs. These are in intimate contact with the meninges and meningeal blood vessels, suggesting signalling through diverse pathways. At GW17, the fissure deepens and begins to fuse, although it is still marked by p73/Reelin+ CRNs. The p73KO mouse illustrates the importance of p73 in CRN for HF formation. In the mutant, Tbr1/Reelin+ CRNs are born in the hem but do not leave it and subsequently disappear, so that the mutant cortex and HC lack CRN from the onset of corticogenesis. The HF is absent, which leads to profound architectonic alterations of the HC. To determine which p73 isoform is important for HF formation, isoform-specific TAp73- and DeltaNp73-deficient embryonic and early postnatal mice were examined. In both mutants, the number of CRNs was reduced, but each of their phenotypes was much milder than in the global p73KO mutant missing both isoforms. In the TAp73KO mice, the HF of the dorsal HC failed to form, but was present in the ventral HC. In the DeltaNp73KO mice, the HC had a mild patterning defect along with a shorter HF. Complex interactions between both isoforms in CRNs may contribute to their crucial activity in the developing brain.

Key words: choroid plexus; cortical hem; meninges; p73; Reelin.

Introduction

Cajal-Retzius neurons (CRN) are early-appearing cells in the cortical marginal zone (MZ). During development, they are the principal source of the glycoprotein Reelin (D'Arcangelo et al. 1995; Ogawa et al. 1995), which is crucial for radial migration and laminar positioning of the neuroblasts that are travelling into the cortical plate (Frotscher, 1998; Tissir & Goffinet, 2003). CRN have various birthplaces, most of

which are located at the interface of telencephalon and choroid plexus (Meyer et al. 2002; Bielle et al. 2005; Meyer, 2010; Roy et al. 2014). The cortical hem is a signalling centre rich in multiple *Wnt* and *Bmp* genes, and is important for patterning of neocortex and hippocampus (HC; Tole & Grove, 2001; Grove et al. 1998; Bulchand et al. 2001; Subramanian & Tole, 2009). CRN have been extensively studied in a variety of species (reviewed by Tissir et al. 2002; Meyer & González-Gómez, 2018b). They reach highest differentiation in the human neocortex at midgestation, where they display unique morphologies before undergoing cell death (Meyer & González-Gómez, 2018a,b). By contrast, the morphology of human and rodent hippocampal CRN is much simpler; they are mono- or bipolar and may survive into adulthood (Del Río et al. 1995, 1996; Drakew et al. 1998; Abraham & Meyer, 2003). They share, however, the same

basic neurochemical profile with neocortical CRN, co-expressing Reelin, transcription factors p73 and Tbr1, the calcium-binding protein calretinin (Soriano et al. 1994; Del Río et al. 1995, 1996; Meyer & Goffinet, 1998; Hevner et al. 2003; Hernández-Acosta et al. 2011), and they are gluta-matergic (Del Río et al. 1995, 1996; Marchionni et al. 2010). The different typology of neocortical and hippocampal CRN raises the question of their origin: Do neocortical and hippocampal CRN arise from the same subdivisions of the hem system? We analysed the early stages of dorsal cortical hem and dorsal HC to establish possible differences with the ventral hem and ventral HC. Unlike in rodents, the human HC is restricted to the temporal lobe, even though initially a hippocampal anlage extends from the frontal to the temporal lobe all along the medial border of the cortex (Macchi, 1951; Rakic & Yakovlev, 1968; Kier et al. 1997). We observed a differential development of the hippocampal fissure (HF) in dorsal and ventral HC, and asked whether CRN might be implicated in this difference.

The HF was first defined by Ramón y Cajal (1911) as the interface between the stratum lacunosum-moleculare of the cornu Ammonis (CA) and the molecular layer of the dentate gyrus (DG), which is crossed by the fibres of the perforant path arising in the entorhinal cortex (Ramón y Cajal, 1909–1911). CRN are critically involved in the pathfinding of the perforant path (Del Río et al. 1997) and are the main transient synaptic targets for ingrowing entorhinal afferents (Supèr et al. 1998). Reelin is expressed not only in CRN but also in hippocampal interneurons (Drakew et al. 1998).

The question of whether CRN contributes to HF formation was prompted by our previous work on the p73KO mouse, which lacks CRN and does not form an HF (Meyer et al. 2002, 2004). We thus compared the development of human dorsal and ventral HF with the development of the murine HF, using the p73-deficient mouse as an experimental model.

TP73 is a p53 family member that controls target genes involved in cell cycle arrest and apoptosis. The p73 protein is an essential regulator of neural stem cell survival and self-renewal (Gonzalez-Cano et al. 2010; Talos et al. 2010) and has a wide range of non-oncogenic roles, e.g. in brain development (Meyer, 2011; Medina-Bolívar et al. 2014; Niklison-Chirou et al. 2016), ciliogenesis (Nemajerova et al. 2016) and fertility (Holembowski et al. 2014; Inoue et al. 2014). The p73 protein can be expressed as the transactivation competent isoform TAp73 or as the N-terminally truncated dominant-negative isoform DeltaNp73, which have opposing pro- and anti-apoptotic roles, respectively (Yang et al. 2000). In addition, there are multiple alternative spliced C-terminus variants (Kaghad et al. 1997). Full-length TAp73alpha seems to be the dominant isoform in biological systems (Vikhreva et al. 2018).

We previously described the cortical phenotype of the global p73KO (Yang et al. 2000) from embryonic stages into adult life (Meyer et al. 2002, 2004; Hernández-Acosta et al. 2011; Medina-Bolívar et al. 2014). While the p73KO

neocortex has a variety of rather mild anatomical defects and an important hydrocephaly, the dominant malformation is the severe hippocampal dysgenesis. We relate here the loss of CRN with the loss of the HF and the subsequent impact on hippocampal morphogenesis. In addition, we examine isoform-specific TAp73KO and DeltaNp73 mutant mice to determine which isoform is dominant in CRN and important for HF formation.

Recent single-cell transcriptome analyses in mouse (Iacono et al. 2018) and human (Fan et al. 2018) demonstrate that CRN expresses a multitude of RNA, the diversity of which suggests an enormous versatility of this cell type, and points to possible interactions with adjacent structures such as the choroid plexus and the meninges. The large size and slow developmental rate of the human brain allow the detection of developmental steps that go unnoticed in the mouse brain. By focusing on the anatomical relationships of the developing hem system and HC in the fetal human brain, we have tried to shed light on the possible mechanisms that lead to the absence of CRN in the p73-deficient mouse cortex and might explain their putative activity in the formation of the HF.

Material and methods

The embryonic and fetal human brains, between 8 and 25 gestational weeks (GW), were from our collection described in previous studies (e.g. Meyer et al. 2000; González-Gómez & Meyer, 2014; Meyer & González-Gómez, 2018a). They were obtained after legal abortions following national guidelines in Spain, under the supervision of the Ethical Committee of the University La Laguna, in accordance with the Declaration of Helsinki, 1964. Written informed consent was obtained from the parents for the use of fetal brains. The brains were fixed in Bouin or Carnoy, embedded in paraffin, and cut in a coronal or, in four cases, in a sagittal plane into 10-μm-thick serial sections.

Mice

The p73$^{-/-}$ animals (Yang et al. 2000) were bred on a mixed C57BL/6 × 129/SvJae background by intercrossing heterozygous mice, and genotyped by polymerase chain reaction (PCR) as described by Hernández-Acosta et al. (2011). Mice were sacrificed under deep anaesthesia at different pre- and postnatal ages following the guidelines of the Ethical Committee of our Institution. The TAp73KO mice (Tomasini et al. 2008) were provided by U.M. and A.N., and the DeltaNp73KO mice (Tissir et al. 2009) were provided by F.T.

Immunohistochemistry

Sections were deparaffinized, hydrated, and boiled in 10 mM citrate buffer (pH 6) for 20 min for antigen retrieval, rinsed in Tris-buffered saline (TBS, pH 7.6, 0.05 M), and incubated in the primary antibodies overnight in a humid chamber. After rinsing, they were incubated in the corresponding biotinylated secondary antibodies (rabbit anti-mouse IgG or goat anti-rabbit IgG; Dako, Glostrup, Denmark), diluted at 1 : 200 in TBS, followed by incubation with avidin-biotin complex (ABC, DAKO) in TBS. Bound peroxidase was

revealed using 0.04% 3,3-diaminobenzidine (Sigma, USA), 0.05% ammonium nickel (II) sulphate and 0.03% hydrogen peroxide in TBS, pH7.6. Sections were dehydrated, cleared and coverslipped using Eukitt (O. Kindler, Freiburg, Germany). Negative controls omitted the primary antibodies. The following primary antibodies were used: a polyclonal antibody anti-p73α (against amino acids (aa) 427–636 of full length p73, 1 : 300, gift of D. Caput; a monoclonal anti-Reelin antibody 142, raised against aa 164–405, gift of A. Goffinet; synthetic peptide within Human Vimentin aa 400 to the C-terminus (acetyl), 1 : 200, Abcam; a rabbit polyclonal antibody against the enzyme glutamate decarboxylase (GAD) (ab49832, 1 : 1000, Abcam; a mouse monoclonal anti-PCNA (proliferating cell nuclear antigen) ([PC10], ab29, 1 : 500, Abcam; a rabbit polyclonal Tbr1 antibody (Millipore, 1 : 100, AB2261); rabbit polyclonal antibodies against calretinin (1 : 3000) and calbindin (1 : 2000) Swant, 7699/4 and CB-38a, respectively; and a mouse monoclonal anti-Human Ki67 (Clone MIB-1, Dako).

Sequential two-colour immunostaining

Antigens were immunolabelled sequentially by using the primary antibody generated in rabbit or mouse. The first antibody was developed using DAB/nickel as chromogen. Thereafter, sections were rinsed in TBS and incubated overnight with the second antibody. After incubation with the biotinylated secondary antibodies and ABC as described above, sections were developed using DAB alone as chromogen.

Double immunofluorescence

Mouse monoclonal anti-Reelin antibody 142 was mixed with rabbit polyclonal anti-Tbr1 antibody and sections were incubated overnight at room temperature. Then, the secondary biotinylated anti-rabbit IgG antibody (1 : 400, Amersham, Arlington Heights, IL, USA) and Alexa Fluor 488 goat anti-mouse IgG (H+L) antibody (1 : 500, A11001, Invitrogen) were incubated for 1 h at room temperature in the dark, followed by incubation with streptavidin Cy3 conjugate (1 : 500, SA1010, Invitrogen) for 1 h. Nuclei were detected by DAPI staining (Chemicon International, Temecula, CA, USA). Slides were rinsed in TBS and then cover-slipped with DABCO (1%) and glycerol-PBS (1 : 1). Negative controls were performed in the absence of primary antibodies. Fluorescence immunosignals were obtained using a Fluoview 1000 laser scanning confocal imaging system (Olympus Optical). Adobe Photoshop Elements 2.0 was used to enhance contrast and brightness of the figures.

Nomenclature

To maintain consistency with our previous work on the same brains, we use the term gestational week (GW) in the sense that gestation begins with ovulation/fecundation. GW thus corresponds to the term 'postconceptional week'.

Results

The cortical hem forms before the appearance of the dorsal HC (GW8–9)

At 8/9 GW, the dorsomedial wall of the cortex is defined by the presence of the incipient cortical plate, or pioneer plate

(Meyer et al. 2000), a layer of densely aggregated neurons that express the early pallial transcription factor Tbr1 (Hevner et al. 2003; Fig. 1A), together with calretinin (CR; González-Gómez & Meyer, 2014). The pioneer plate is widest in the lateral parts of the cortex and decreases in width as it approaches the hippocampal anlage and the cortical hem. The cortical hem is marked by the intense calbindin (CB) immunoreactivity in its neuroepithelium and wide marginal zone (MZ; Meyer, 2010; González-Gómez & Meyer, 2014; Roy et al. 2014). There was no clear boundary between hem and hippocampal anlage, but rather a decreasing gradient of CB positivity from ventral to dorsal (Fig. 1D). The hem gave rise to large numbers of CRN, which near their birthplace expressed Tbr1 (Fig. 1A,H), Tbr2 (Fig. 1B,G), p73 (Fig. 1C) and often CB (Fig. 1D). CRN became CR[+] and Reelin[+] (Fig. 2C,D) only after reaching the MZ of the prospective cingulate cortex (Meyer et al. 2002), where they stopped to express Tbr2 (Fig. 1B,G). The time point of 8–9 GW represented the peak production of hem-derived CRN, as indicated by comparing the numbers of Reelin[+] CRN at previous preplate stages (Fig. 2A–D). Remarkably, there was no recognizable HF, and CRN seemed to migrate taking a dorsal and then lateral route into the neocortex. The CR/Tbr1^{+} pioneer plate (González-Gómez & Meyer, 2014) was continuous with a CR[+] (Fig. 1E) and Tbr1^{+} (Fig. 1F) cell group in the HC anlage, which became less compact ventrally in the prospective dentate area (Fig. 1E,F). The ventral progression of the Tbr1^{+} pioneer plate was slightly more advanced in the fetus of Fig. 1A,B,F,D, compared with the fetus in Figs 1C–E and 2C. This may be due to an age difference of a few gestational days (also compare the increase in differentiation of the pioneer plate between Fig. 2C and D). At 10 GW (Fig. 2D), the CR[+] cell group in the prospective dentate area had gained prominence and even seemed to extend fibres towards the fimbria, which had appeared in the ventral-most part of the hippocampal anlage. Of note, at these stages we did not detect immunoreactivity for Prox1, a marker of dentate granule cells (Stergiopoulos et al. 2015). A CB[+] Ammonic plate appeared only at 12 GW (Fig. 2F), ventral to a prominent callosal sulcus; its neurons had a pyramidal shape. At 12 GW (Fig. 2E), the dentate area was populated by many small CR^{+} neurons that may represent the first granule cells, although clear positivity for Prox1 was observed only at 13 GW. The large CR^{+} neurons of earlier stages (9–10 GW) were no longer observed and may be transient. The fimbria had now increased in size and contained both CR[+] and CB[+] fibres. In turn, the cingulate cortex had lost the intense CR immunoreactivity of the pioneer plate stage and was developing a proper cortical plate.

At 12 GW, the production of CRN in the dorsal hem was no longer evident, although a few Reelin[+] CRN were still visible along the fimbria (Fig. 2D). The MZ was slightly enlarged at the interface of the Ammonic plate and dentate area, representing an incipient HF containing CRN.

However, the number of CRN was higher in the MZ of the callosal sulcus between the prospective cingulate cortex and the hippocampal anlage.

Topographical relationships between cortical hem, choroid plexus and hippocampus

The close anatomical relationship between cortical hem, CRN and choroid plexus reflects their common origin from the telencephalic dorsal midline (Imayoshi et al. 2008). In addition to the well-known cortical (dorsal) hem, there is also a ventral hem providing CRN for the ventral HC (Abraham et al. 2004). In addition, at 9/10 GW we identified a distinct sector of the choroid plexus/hem complex located at the caudalmost extension of the choroid plexus (the future glomus choroideus in the atrium of the lateral ventricle before bending ventrally into the temporal horn). Here,

the choroid plexus branched into differentiated dorsal (parietal) and still immature ventral (temporal) folds, and was directly interposited between dorsal and ventral hem (Fig. 3A). Just caudal to the future glomus choroideus, dorsal and ventral hem merged, forming a caudal hem in the form of a thin sheet of tissue (Fig. 3B), all expressing high levels of CB, and giving rise to numerous CB^+ (and $p73^+$, Abraham et al. 2004) CRN (Fig. 3C). As they moved away from the hem, CRN began to express CR (they may express both CR and CB, Verney & Derer, 1995). Intensely CB^+ folds of the choroid plexus were in close contact with the dorsal hem and the adjacent CB^- neuroepithelium, where the MZ was densely populated by CB^+ CRN (Fig. 3C). Figure 3E shows the caudal hem at 10 GW; the cells dividing at this time point may represent the first migration of the dorsal and ventral DG from their origins in the primary dentate neuroepithelium toward the pial surface. This
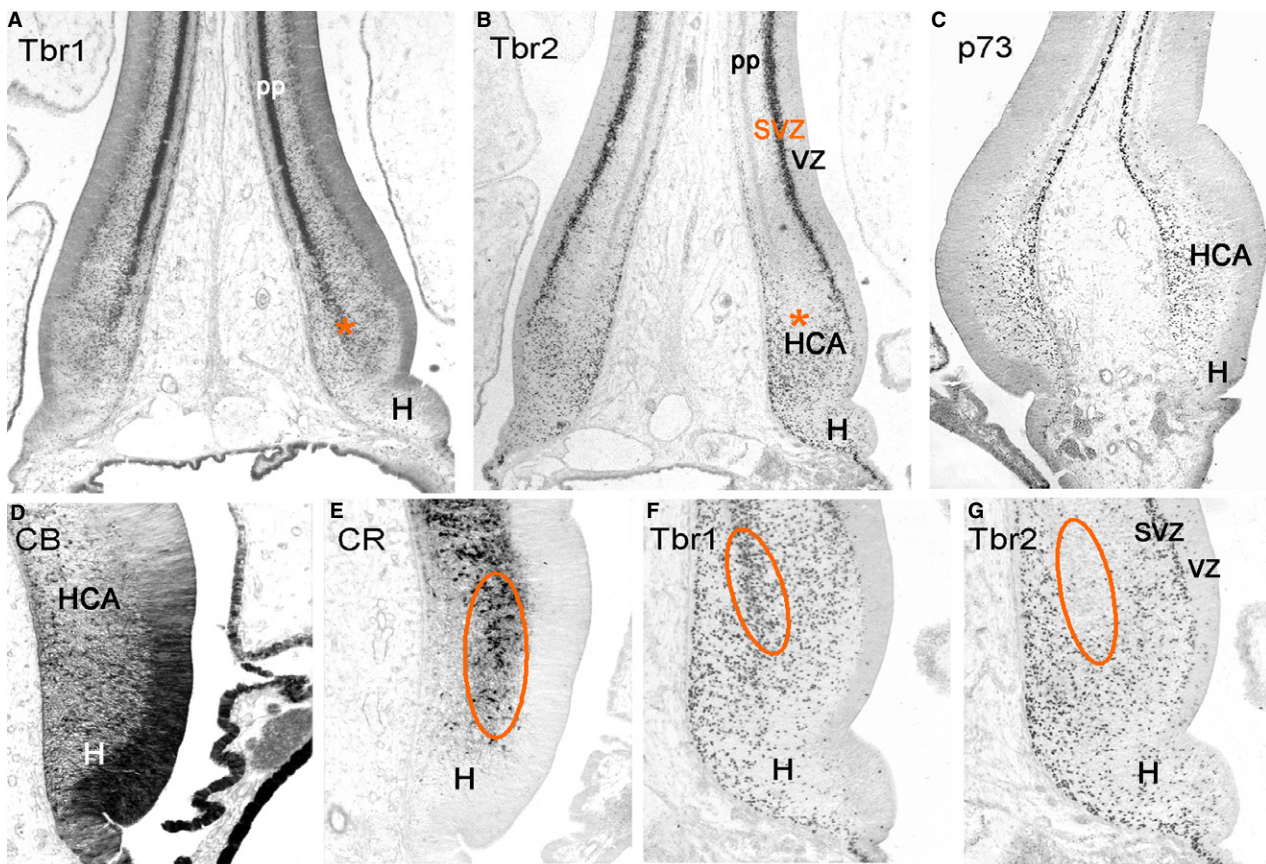

Fig. 1 The dorsal cortical hem (H) at 8/9 GW is the birthplace of CRN. (A) Tbr1 strongly stains postmitotic CRN in the marginal zone (MZ) of the medial cortex, and pioneer neurons in the pioneer plate (pp). The red asterisk marks the area shown in detail in (F). (B) Tbr2 marks intermediate progenitor cells in the subventricular zone (SVZ) and CRN progenitors in the cortical hem and in the medialmost MZ. (C) p73 specifically marks CRN in the hem and MZ of the pioneer plate, and the choroid plexus epithelium. (D) CB expression at higher magnification in the cortical hem is in the neuroepithelium and in CRN, which are CB^+ before switching to CR expression in the MZ. The choroid plexus is also intensely CB^+. (E) An adjacent section immunostained for CR shows the first neurons in the prospective hippocampal area (HCA), which become more dispersed close to the hem. Compare with (F). $Tbr1^+$ neurons have a similar distribution, suggesting that these are the first representatives of Ammonic and dentate plates (encircled in E,F,G). (G) Tbr2 represents CRN progenitor cells in the hem overlapping with intermediate progenitors in the SVZ of the hippocampal anlage. The $Tbr1^+$ and CR^+ 'plate' is $Tbr2^-$ (encircled area in E,F,G). VZ, ventricular zone.
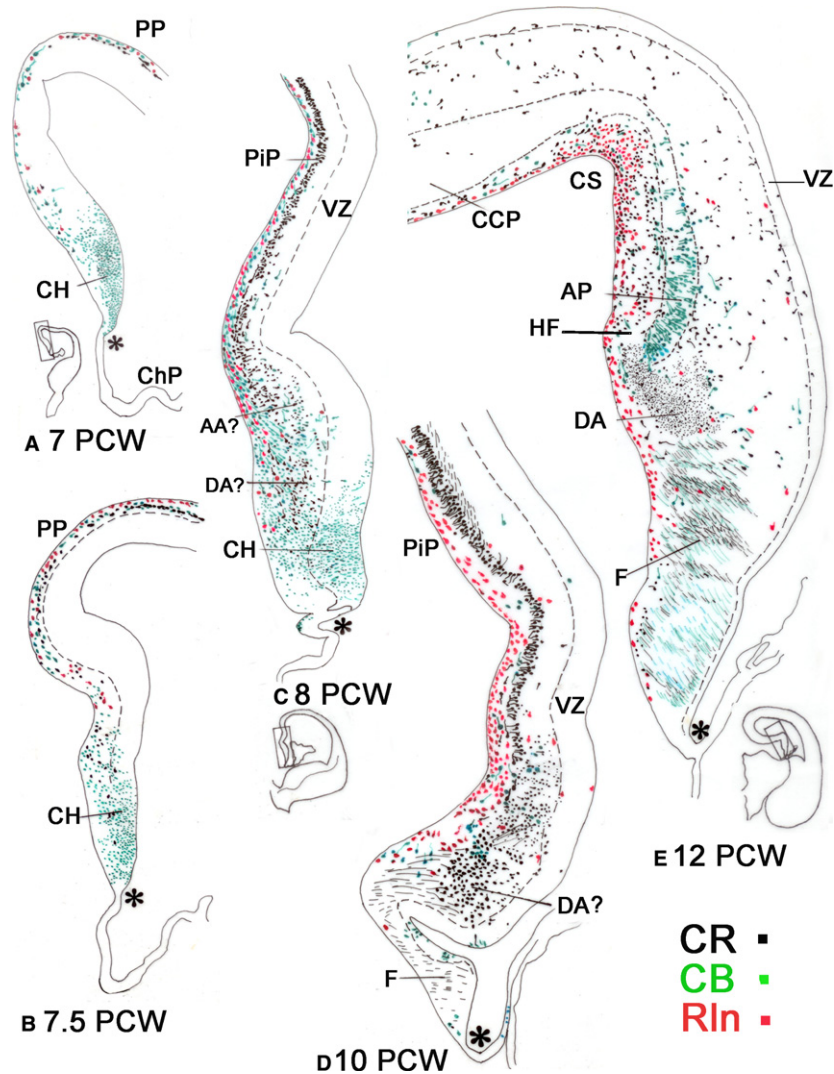
Fig. 2 From the cortical hem to the dorsal hippocampus. Camera-lucida drawings from adjacent sections individually stained for Reelin, calretinin and calbindin (see colour code) summarize the events that lead from the first outmigration of presumptive CRN from the cortical hem at 7 GW (A), their increase in number in (B) 7.5 GW, to the maximum presence of CRN shortly before the ouvert appearance of the hippocampus at 8/9 GW (C). At this stage (represented in Fig. 1) the CR+ pioneer plate has formed in the dorsomedial cortex and advances toward the hem. (D) At 10 GW, the pioneer plate reaches the hippocampal anlage. Notice the first axons arising from the more advanced dorsal levels taking a lateral course. In the prospective dentate anlage (DA), large CR+ neurons seem to give rise to fibres that are directed towards the fimbria (F). Of note, CB expression is no longer in the hem when the HC emerges. (E) At 12 GW, the Ammonic plate (AP) appears as a CB+ plate populated by radially oriented pyramidal cells. In the dentate anlage, small CR+ cells predominate. The fimbria is larger and contains both CR+ and CB+ fibres. All drawings are at the same scale. The asterisks indicate the boundary between hem and fimbria, respectively, with the choroid plexus attachment. AA, Ammonic anlage; CCP, cingulate cortical plate; CH, cortical hem; CS, callosal sulcus; DA, dentate anlage; F, fimbria. PiP, pioneer plate; PP, preplate.

interpretation was confirmed at 13 GW, when two CR+ secondary migratory streams (CR marks immature granule cells; CB is expressed later; Brandt et al. 2003; Abrahám et al. 2009) converged at a level caudal to the caudal hem (Fig. 3F), where dorsal and ventral HC merged. The junction of dorsal and ventral DG led to a single caudal DG (Fig. 3G). By contrast, at levels rostral to the glomus choroideus, dorsal and ventral hem/HC became increasingly separated by the growing basal ganglia. Figure 3D shows a sagittal view at 14 GW, when dorsal and ventral HC appeared almost like mirror images when they were connected by a lamina of choroid tissue (choroid stem cells, according to Bayer & Altman, 2005). Both fimbriae were connected with this choroid lamina through a thin membrane, the future taenia of the fornix/fimbria.

Ammonic and dentate anlagen of the dorsal HC

The early development of CRN in the human ventral HC has been described in previous work (Abraham et al. 2004).

Much less is known about the developmental changes in the dorsal HC after 12 GW and its transformation into the indusium griseum (IG). At 13 GW, the dorsal HC displayed an Ammonic plate formed by CB$^+$ pyramidal cells (Fig. 4C) and a wide MZ, where an outer and inner MZ could be distinguished. Reelin$^+$ CRN resided mainly in the outer MZ (Fig. 4D). Ventral to the Ammonic plate was a cluster of small CR$^+$ granule-like cells (Fig. 4B,E), continuous with a proliferating secondary dentate matrix (Altman & Bayer, 1990a,b; Fig. 4A). Immunostaining with Prox1 confirmed the granule cell identity in the ventral part of the dentate anlage (Fig. 4F). The more dorsal part was only CR$^+$ and may represent early granule cells. The larger CR$^+$ cells of earlier fetal stages, perhaps transient pioneer cells, were no longer observed (Human mossy cells of the hilus do not express CR, Seress et al. 2008). The MZ between Ammonic plate and dentate anlage was slightly invaginated and had a triangular shape; it was populated by Reelin$^+$ CRN
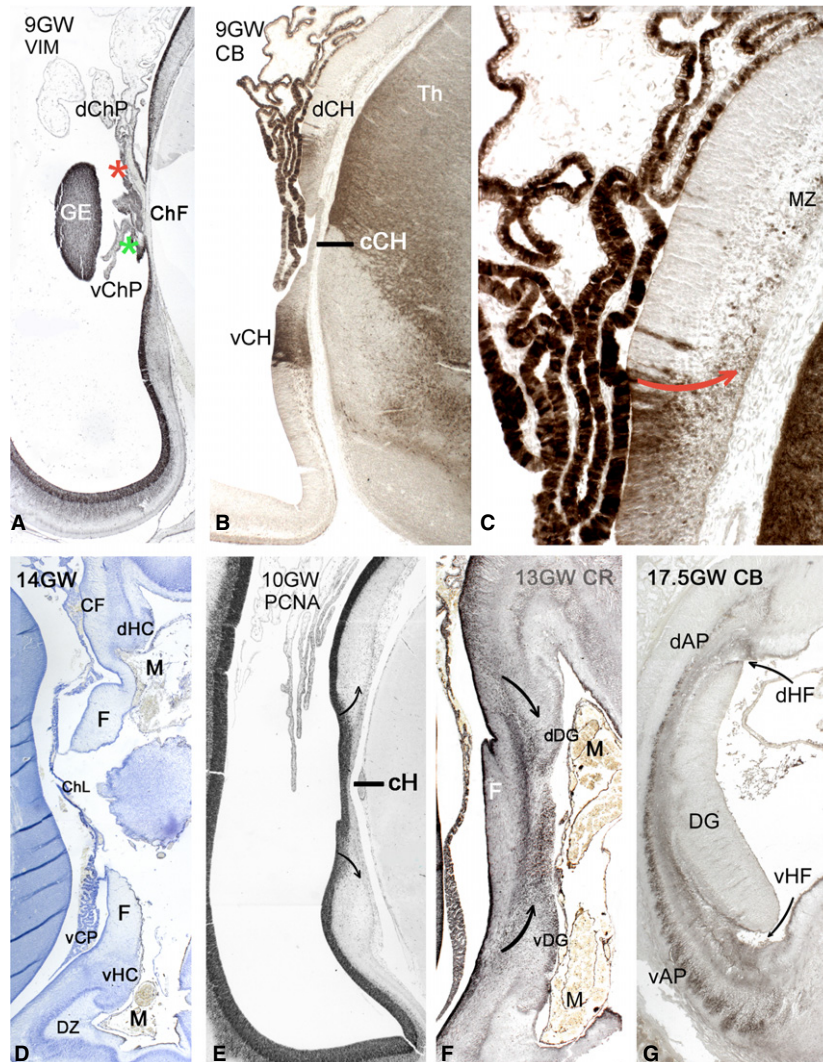

Fig. 3 The caudal cortical hem and the junction of dorsal and ventral HC. (A) 9 GW. The future glomus choroideus is interposed between dorsal and ventral hem and gives rise to dorsal (dChP) and ventral (vChP) folds. The roots of the dChP (red asterisk) and the vChP (green asterisk) are connected in the choroid fissure (ChF). Vimentin stains radial glia and cells in the roots of the ChP. (B) The junction of dorsal and ventral cortical hem (dCH, vCH) occurs at the caudal cortical hem (cCH), which is just caudal to the section in (A) Both hems and the ChP are intensely CB-positive. (C) Higher magnification of the close attachment of the ChP to the dorsal hem in (B). CB$^+$ CRN spread from the caudal hem into the adjacent marginal zone (MZ) (red arrow). (D) 14 GW, sagittal section, Nissl. Dorsal and ventral HC (dHC, vHC) are similarly developed and connected by a choroid lamina (ChL). In the dHC, callosal fibres (CF) are aggregated near the ventricular zone. In the vHC, the meninges (M) target the ventral HF and diffuse zone (DZ). (E–G) The fusion of dorsal and ventral dentate gyrus (DG), at 10 (E), 13 (F) and 17.5 (G) GW. In (E) PCNA marks the primary dentate migration (arrows); in (F) calretinin marks the subpial migration of dentate progenitors (arrows). In (G) the fused dentate gyrus is not yet CB$^+$. CB marks the Ammonic plate of dorsal (dAP) and ventral (vAP) HC. Arrows point to the dorsal (dHF) and ventral (vHF) hippocampal fissure. F, fornix, GE, ganglionic eminence, Th, thalamus.

(Fig. 4D), which were also positive for CB (Fig. 4C) and CR (Fig. 4E), and indicated an incipient HF. The general arrangement of Ammonic plate and dentate anlage in dorsal HC and ventral HC at 13/14 GW was similar, although the HF in the ventral HC was much larger, increasing during the following weeks (see below). CRN were not numerous in the dorsal HF, and even the future callosal sulcus contained more CRN (Fig. 4B). Of note, the dividing cells emerging from the VZ around the dentate notch (asterisk in Fig. 4A,B) were more numerous than the comparatively few Prox1^{+} prospective dentate granule cells and included many GFAP[+] astrocytes (not shown) for the fimbria/fornix and the already forming corpus callosum (CC). The first callosal fibres were recognizable at 13 GW as an immuno-negative tract in the medial subventricular/intermediate zone, which crosses the midline between the dentate anlage and the fimbria during the following weeks (curved arrow in Fig. 4B).

Here, we want to point out an observation made in the nine examined cases between 13 and 16 GW, which we believe represents a consistent developmental feature rather than a tissue artefact. As we did not remove the meninges, the distinct distribution of the meninges in the developing dorsal vs. ventral HC was preserved across the stages. In the ventral HC, the bulk of meninges and meningeal blood vessels was directed towards the ventral HF, whereas in the dorsal HC the meninges pointed to the site of the future CC between dentate anlage and fimbria/fornix, but clearly not to the dorsal HF (Fig 4A,B). As the meninges are involved in brain development via multiple signalling pathways (discussed below), they may actually instruct both the deepening of the ventral HF and the formation of the CC.

The formation of the indusium griseum

The first fibres of the CC appeared at 13 GW in the rostral telencephalon in the commissural plate dorsal to the septal nuclei (Rakic & Yakovlev, 1968). At 15/16 GW (not shown), the CC had not advanced significantly in a caudal direction, and the acallosal dorsal HC maintained basically the same morphology and its predominantly vertical orientation described above for 13 GW (Fig. 4A,B). At 17.5 GW, the CC had reached more caudal levels (the sections in Fig. 5 are all at a midfrontal level) and transformed the acallosal dorsal HC into a supracallosal indusium griseum. The expansion of the CC led to a deepening of the callosal sulcus and a re-positioning of the dorsal HC in a horizontal plane, covering the CC (Fig. 5A). The now supracallosal HC/IG maintained features of an Ammonic plate formed by CB^{+} pyramidal cells, and a dentate area dominated by small CR^{+} neurons, possibly representing granule cells (Fig. 5A,C,F). Long vimentin[+] radial glia fibres arose in the SVZ underlying the Ammonic plate, traversed the callosal fibres and ran radially into the Ammonic plate (Fig. 5B, white arrow). In the

adjacent dentate area, a central 'hilus' was densely filled with vimentin[+] glia (Fig. 5B), containing also many mitotic cells (Fig. 5E) and some small CB^{+} neurons (Fig. 5F). Reelin[+] CRN were numerous in the callosal sulcus, in the MZ of the Ammonic plate, and in the MZ between Ammonic and dentate areas, indicating the persistence of a small dorsal HF (Fig. 5D). At this age, the midline meninges and meningeal blood vessels were particularly prominent. They were even directly attached to the medial tips of the dentate area (Fig. 5A,B) and were also in closely contact with the CC, features that were no longer observed at later stages (Fig. 5G). At 23 GW (Fig. 5G) and 25 GW (not shown), there were no signs of involution of the dorsal HC, but rather of differentiation such as a better definition of lamination in both Ammonic (Fig. 5H) and dentate (Fig. 5G) parts. It is thus conceivable that the human dorsal/supracallosal HC does not undergo regression but stops increasing in size after the appearance of the CC to evolve into an IG. Due to the lack of older material we were unable to determine whether the IG undergoes involution at later stages of development.

CRN and the widening of the ventral hippocampal fissure

The main steps in the development of the ventral HC were defined by Abraham et al. (2004), but little attention was paid to specific aspects of HF formation that are different between dorsal and ventral HC. In short, after the disappearance of the ventral hem and during the protracted time of dentate granule cell production, p73/Reelin[+] CRN for the ventral HF derives from a secondary birthplace near the dentate notch (Fig. 5E), migrates along the fimbria/dentate glial scaffold to the pial surface, and populates the growing HF and dentate MZ (Abraham et al. 2004).

As mentioned above, already at 13/14 GW, meninges and meningeal vessels invaded the ventral HF (Fig. 3D), which became a deep, wide opening diffusely filled with CRN, loose pial tissue and small blood vessels (the diffuse zone of Humphrey, 1967), particularly prominent at 15–16 GW. This process was missing in the dorsal HC. Fig. 6A,B shows that the diffuse zone stage concurred with the formation of the tertiary matrix and secondary glial scaffold (Fig. 6C) of the lateral DG adjacent to the CA fields, where a dentate molecular layer was also beginning to form (Fig. 6F,H). During this short transient period, p73[+] CRN appeared directly to surround meningeal microvessels (Fig. 6F,H). Unlike in neocortex, where we detected proteins such as nitric oxide synthase and CXCR4 in CRN (Meyer & González-Gómez, 2018a,b), the immunostaining in HC was too diffuse to be specific. Importantly, the neuronal population in the diffuse zone included Reelin[+] interneurons which were p73[−] (Fig. 6G), and may belong to the many GAD[+] interneurons in the HF (Fig. 6D).This period of intense meningeal invasion of the HF was basically over by 17 GW (Fig. 6I,J), when
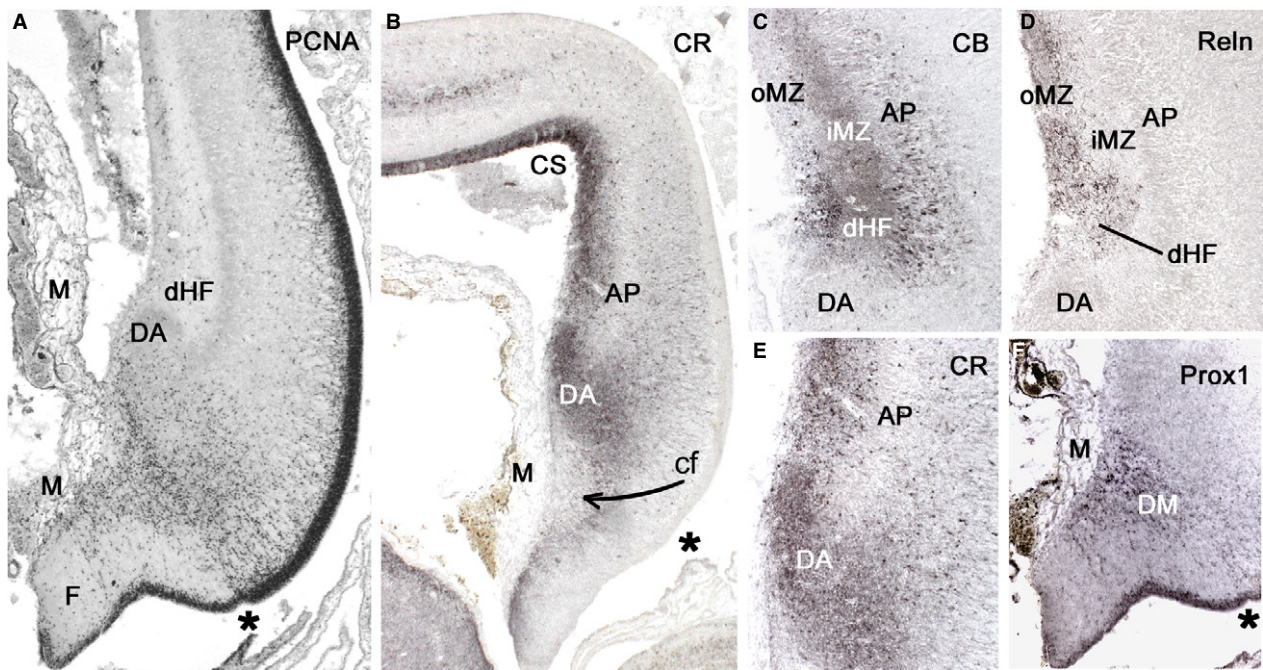
Fig. 4 The dorsal hippocampus at 13 GW. (A) PNCA shows a migration stream of dividing cells from the dentate notch (asterisk) to the pial surface, closely contacted by the meninges (M). DA, Dentate anlage. (B) Calretinin (CR) marks small neurons in the DA and CRN in the marginal zone of the Ammonic plate (AP). Callosal fibres (cf) are assembled between DA and fimbria (F), and the arrow indicates their prospective path in the following weeks. (C) Calbindin (CB) marks pyramidal cells in the AP and their processes in the inner marginal zone (iMZ), as well as CRN in the HF and outer marginal zone (oMZ). Compare with (D): Reelin marks CRN in the oMZ and in the rudimentary dorsal hippocampal fissure (dHF). (E) The same area with CR shows a negative AP, a positive DA, and CRN in the dHF. (F) The dentate migratory (DM) path with Prox1. CS, Callosal sulcus.

the HF started to fuse, and meninges remained at the outer part of the fissure where it was still open. The HF continuously deepened and fused during the following weeks, separating the molecular layer of the DG and the stratum lacunosum-moleculare of subiculum and CA1. CRN followed the deepening HF (Abraham et al. 2004). Even after the closure of the HF, blood vessels perfusing the HC took the initial route of the HF. Like all perforating vessels, they were surrounded by the pia of the Virchow-Robins spaces, such that pial mesenchyme remained in the fused HF.

p73 in CRN of the developing hippocampal fissure

Since p73 is expressed in virtually all CRN deriving from the hem system, we studied a mouse model, first by defining the expression of p73 in the mouse hem system, secondly by analysing the hippocampal defect of the p73KO mouse, and thirdly by comparing the defects of isoform-specific p73KO mice. Figure 7A schematically represents the two main isoform classes of the p73 protein that result from different promoter usage of the p73 gene at the N-terminus. The TAp73 isoform is a transcription factor, whereas DeltaNp73 acts as a dominant-negative transcriptional inhibitor. The C-terminus undergoes alternative splicing giving rise to p73 alpha, beta, gamma plus additional isoforms. The arrows indicate the epitope of the p73 antibody used,

which recognizes p73α but does not distinguish between N-terminal isoforms.

Importantly, the global p73KO mouse missing all isoforms lacks CRN in cortex and hippocampus (Meyer et al. 2004). However, confocal imaging using antibodies to detect the CRN-specific coexpression of Reelin and Tbr1 (Fig. 7B) showed that CRN were born in the hem, but did not migrate into the HF or farther into the cortex, and possibly died almost immediately. In E15 wild type (wt) mice, a dorsal hem with numerous CRN (Fig. 7C,D) was continuous more caudal to the ventral hem, a thin tissue where CRN were more prominent slightly later at E15.5 (Fig. 7E, inset). At the caudal end of the HC, the HF was vertically oriented, and the dentate gyrus was medial to the HF (Fig. 7F). As shown in Fig. 7D, the layer of CRN around the ventral tip of the HC seemed to be directly continuous with the choroid plexus epithelium.

In contrast to the global p73KO mouse, which completely lacked CRN in the cortical MZ (Fig. 7J), the embryonic (E14) TAp73KO mouse had a severely reduced number of CRN (Fig. 7H), whereas in the E14 DeltaNp73KO mouse the CRN defect was more subtle and may combine with a general upregulation of Reelin (Fig. 7I), compared with the E14 wt mice (Fig. 7G).

We followed the development of the global p73-deficient HC from E15 into adulthood and found that the initial
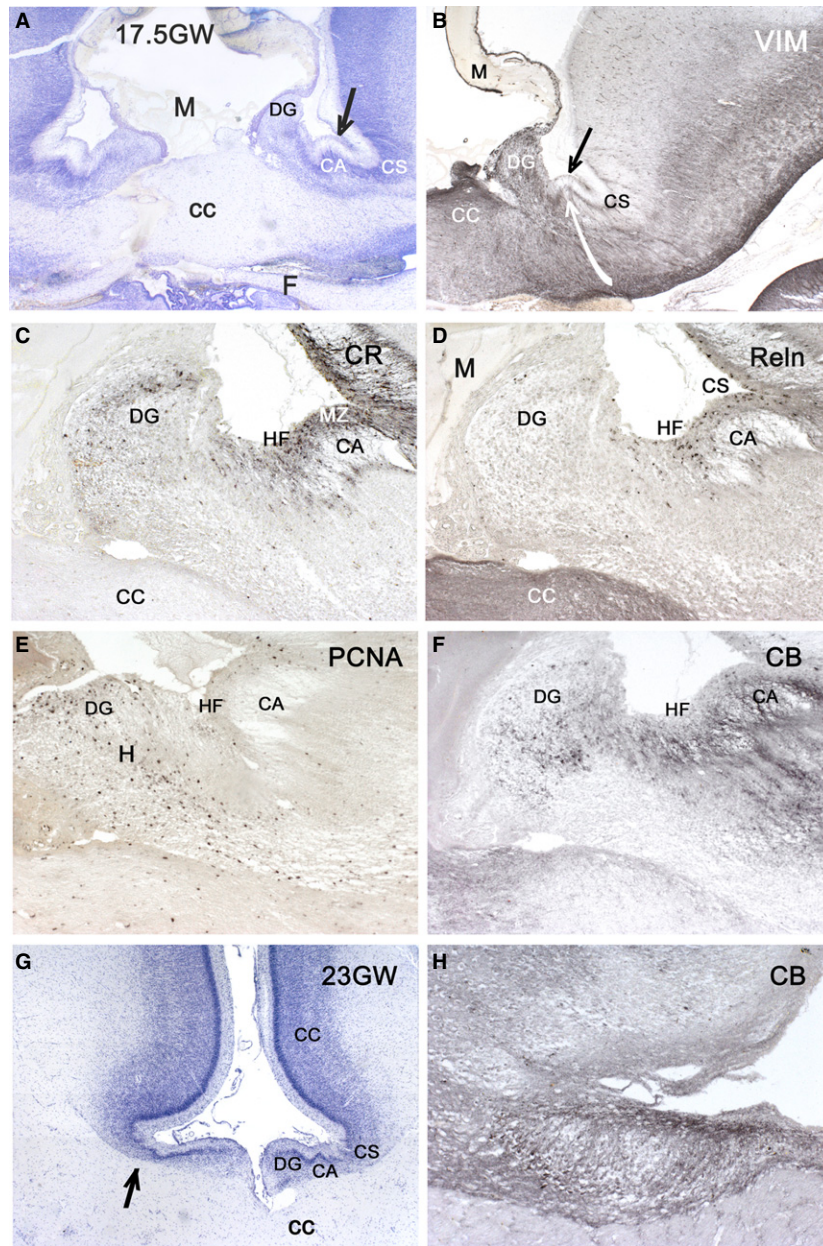
Fig. 5 The formation of the indusium griseum. (A–F) 17.5 GW. (A) A parallel Nissl-stained section showing the corpus callosum (CC) crossing the midline in close contact with the meninges (M). All sections are at a midfrontal level. The arrow in (A) points to the same structure in (B). (B) Vimentin marks radial glial fibres in the cornu Ammonis (CA) field of the indusium griseum, traversing the fibres of the CC (white arrow). In the dentate part (DG), astrocytes lack a radial organization. (C) Expression of calretinin (CR) in CRN of the CA marginal zone (MZ) and dorsal hippocampal fissure (HF), and in granule cells of the dorsal dentate gyrus (DG). (D) Reelin in CRN of MZ and the rudimentary HF. (E) PCNA in a stream of dividing cells from the hilus (marked as H) to the pial surface of the DG. (F) Calbindin marks pyramidal cells in CA and a group of small cells in the DG. (G,H) 23 GW. (G) Nissl, showing laminar refinement of the IG. The arrow points to the CA field of the IG, shown in (H). (H) CB in pyramidal cells with laminar arrangement. CC, cingulate cortex; CS, callosal sulcus.

defect was the inability of embryonic CRN to leave the hem and assemble in the HF (Fig. 8A,B). At postnatal day 9, CRN were still prominent in the wt HF but were absent in the p73KO mouse (Fig. 9 C,D). Even though Reelin⁺ interneurons were present in the strata oriens and lacunosum-moleculare of CA1 and the dentate molecular layer (Fig. 8D,G),

they were unable to rescue the formation of the HF. Thus p73 is the decisive factor that determines whether the HF develops.

How does the HC develop without a HF? The adult p73KO mouse had all the main components of a wt HC: subicular complex (subiculum and presubiculum), cornu
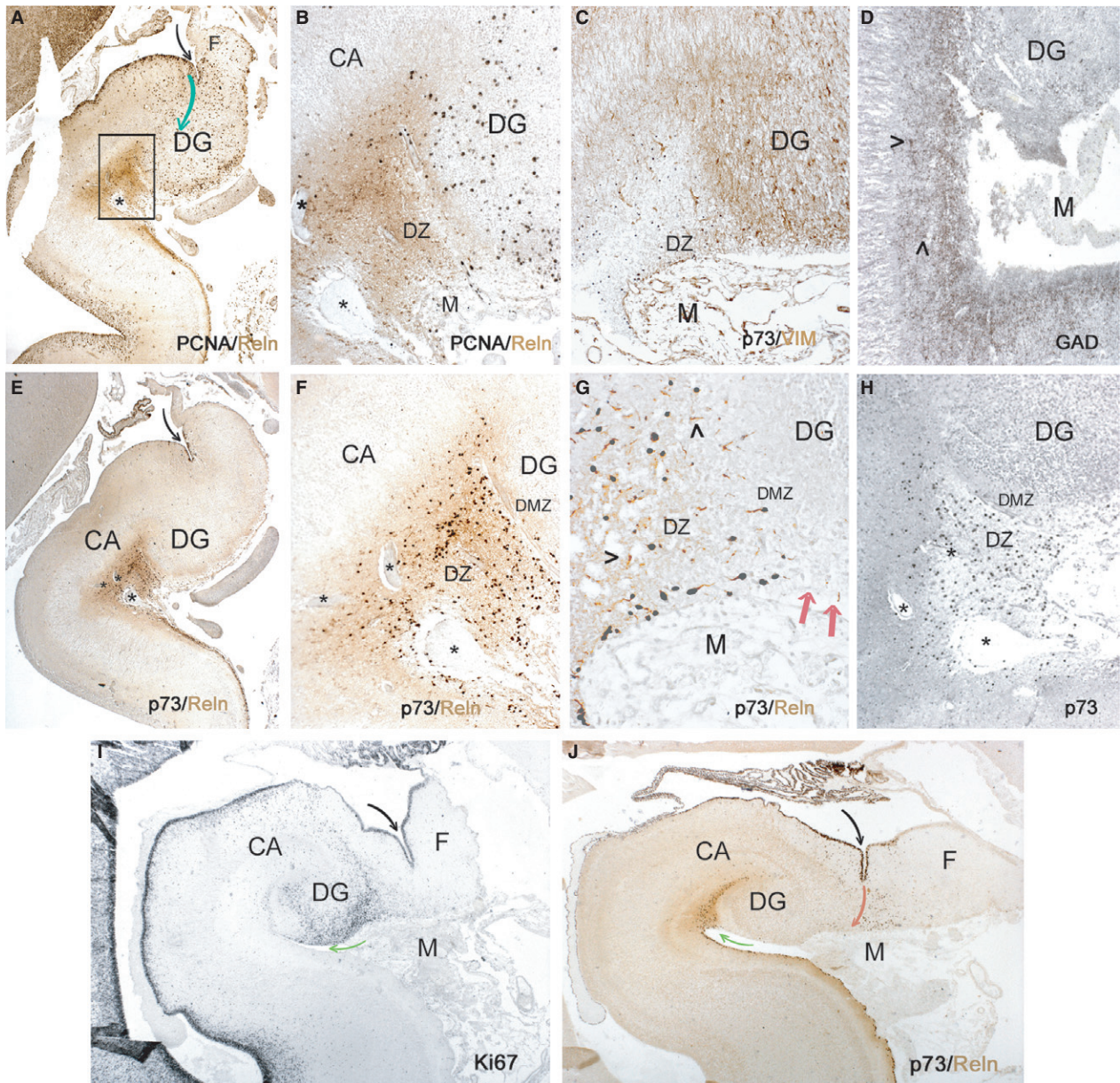
Fig. 6 The opening of the ventral hippocampal fissure. (A–H) 15GW. (A) Panoramic view of the open hippocampal fissure (HF), double-stained with PCNA and Reelin to visualize the dentate migratory stream (green arrow) from the neuroepithelium near the dentate notch (black arrow) into the proliferating dentate gyrus (DG). The rectangle is shown at higher magnification in (B). (B) Reelin is highly expressed in the diffuse zone (DZ), the wide marginal zone (MZ) of the ventral HC. Meninges (M) and associated blood vessels enter the diffuse zone. The asterisks in (A,B,E,F) mark the same vessels. (C) The same area, with vimentin defining the secondary glial scaffold of the DG, and p73 (in black) visualizing CRN in the DZ. (D) GAD[+] interneurons are numerous in the MZ of the HF. The open arrowheads point to clearly visible somata within the intensely stained neuropil. (E) Panoramic view of HF, double-stained with p73 and Reelin. Late-appearing CRN arise from a p73[+] area around the dentate notch (black arrow). (F) Higher magnification of (E) reveals the wide, highly vascularized DZ. (G) A high power view shows that Reelin and p73 co-localize in CRN in the DZ, whereas interneurons express only Reelin (open arrowheads). Only the DG adjacent to the DZ has a few CRN in the dentate MZ (DMZ), whereas the medial DG does not yet have a DMZ, and no CRN (red arrows). (H) p73[+] CRN closely assemble around meningeal vessels. (I,J) 17 GW: The fused, deepening HF. In (I), Ki67 reveals mitotic cells in the hilus, medial DG and dentate migratory stream. The black arrow points to the dentate notch, the green arrow to the superficial, open HF. (J) Double-stained p73/Reelin CRN follow the deepening HF separating CA and DG. The black arrow points to the p73[+] dentate notch, the red arrow indicates the proposed route of late-appearing CRN, and the green arrow marks the superficial, open HF. F, Fimbria.

Ammonis and DG. Of these, the CA fields were the most severely affected, with CA1/2 presenting undulations and sulcus-like depressions. Reelin[+] interneurons were abnormally clustered in the stratum lacunosum–moleculare of the dilated CA regions and the adjacent molecular layer of the DG (Fig. 8G). The medial blade of the dentate gyrus
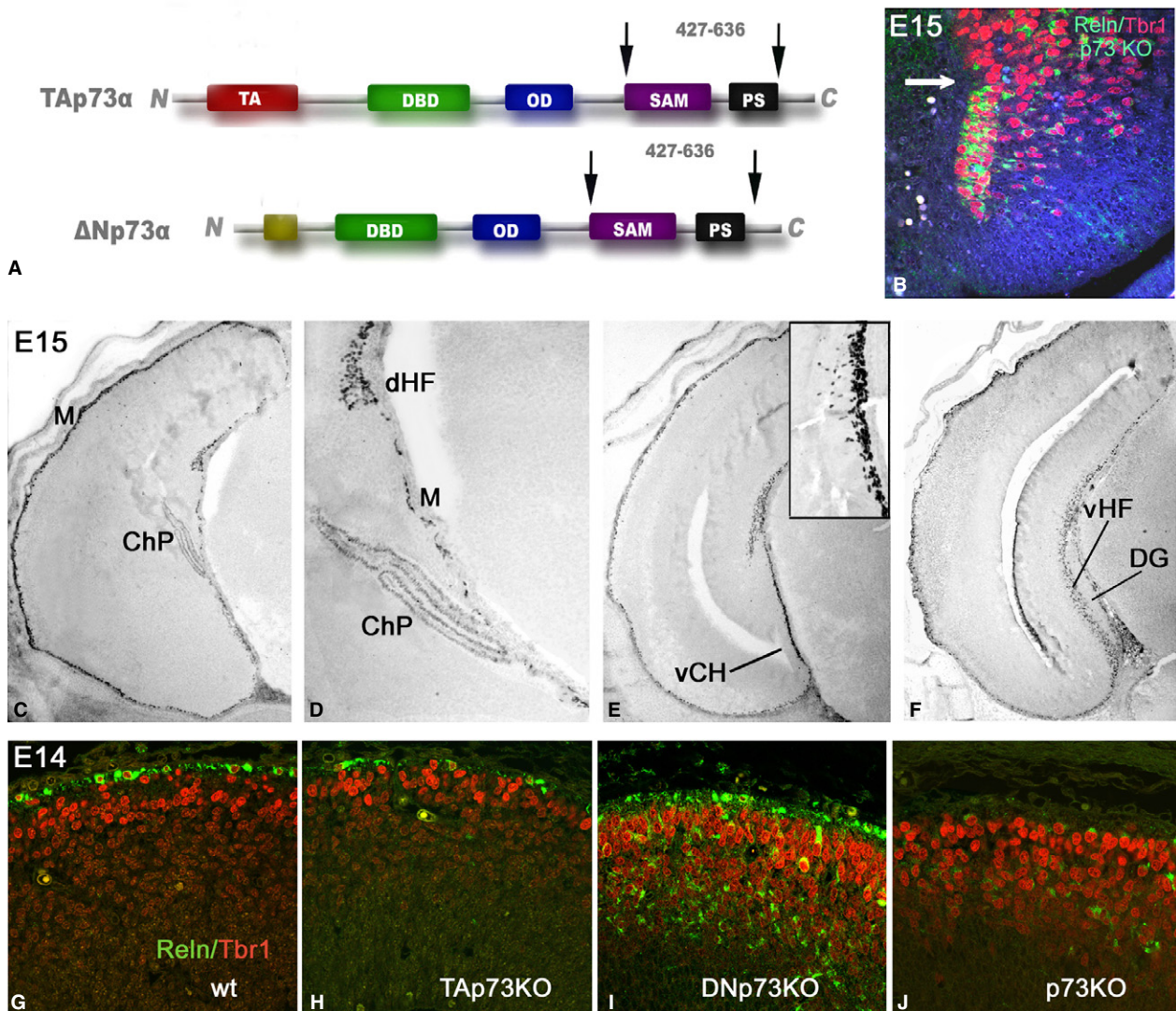
Fig. 7 p73 in the embryonic mouse brain. (A) Schematic representation of the two N- terminal isoforms of the p73α protein, TAp73α and DeltaNp73α. The arrows point to the epitope of the antibody used in this study, which was raised against the C-terminus of p73α and does not distinguish TAp73 and DeltaNp73 isoforms. (B) Confocal microscopy of the cortical hem in a global p73KO mouse at E15. Tbr1 (red), and Reelin (green) label CRN originating in the hem, which do not migrate dorsally and do not assemble in the aborted HF (white arrow). (C–F) Different rostro-caudal levels of the HF in an E15 wildtype embryo. The p73 antibody stains CRN and choroid plexus. (D) CRN of the dorsal HC appear to be directly continuous with the p73+ epithelial cells of the choroid plexus. (E) The arrow points to the ventral cortical hem (vCH), where CRN for the ventral HF are generated. The inset shows the vCH at E15.5, when the outmigration of p73+ cells reaches its maximum. (F) Caudal HF which has a vertical orientation. Notice that in this embryo the meninges (M) were not removed and are in close contact with CRN. (G–J) Confocal images of the dorsal cortex at E14 with Tbr1 in red and Reelin in green. (G) Wildtype (wt). (H) TAp73KO, with severely reduced CRN density. (I) DeltaNp73KO, where CRN are slightly less numerous. (J) Global p73KO, with complete absence of CRN.

was absent or abnormally curved toward the pial surface (Fig. 8F). Nonetheless, the main intrinsic pathways were preserved: the CB+ mossy fibre pathway from the DG to CA3 was present, though also abnormally undulated (Fig. 8H). The mossy cells in the hilus, which in the mouse express CR (Fig. 8E,F), maintained a relatively normal position and sent their axonal plexus into the inner, supragranular molecular layer of the DG, even though there seemed to be some axonal spread into the subiculum (Fig. 8F). Our ongoing tracing studies will determine to what extent

extrinsic connections are affected, in particular the perforant path.

In view of the extreme hippocampal malformation the question is whether the p73KO HC is functional. Although we tried to apply the most common memory and avoidance tests (data not shown), the animals were unable or too passive to react to stimuli such as electric shocks and had to be removed from the tasks. The only memory item they seemed to retain was where to find water and food.
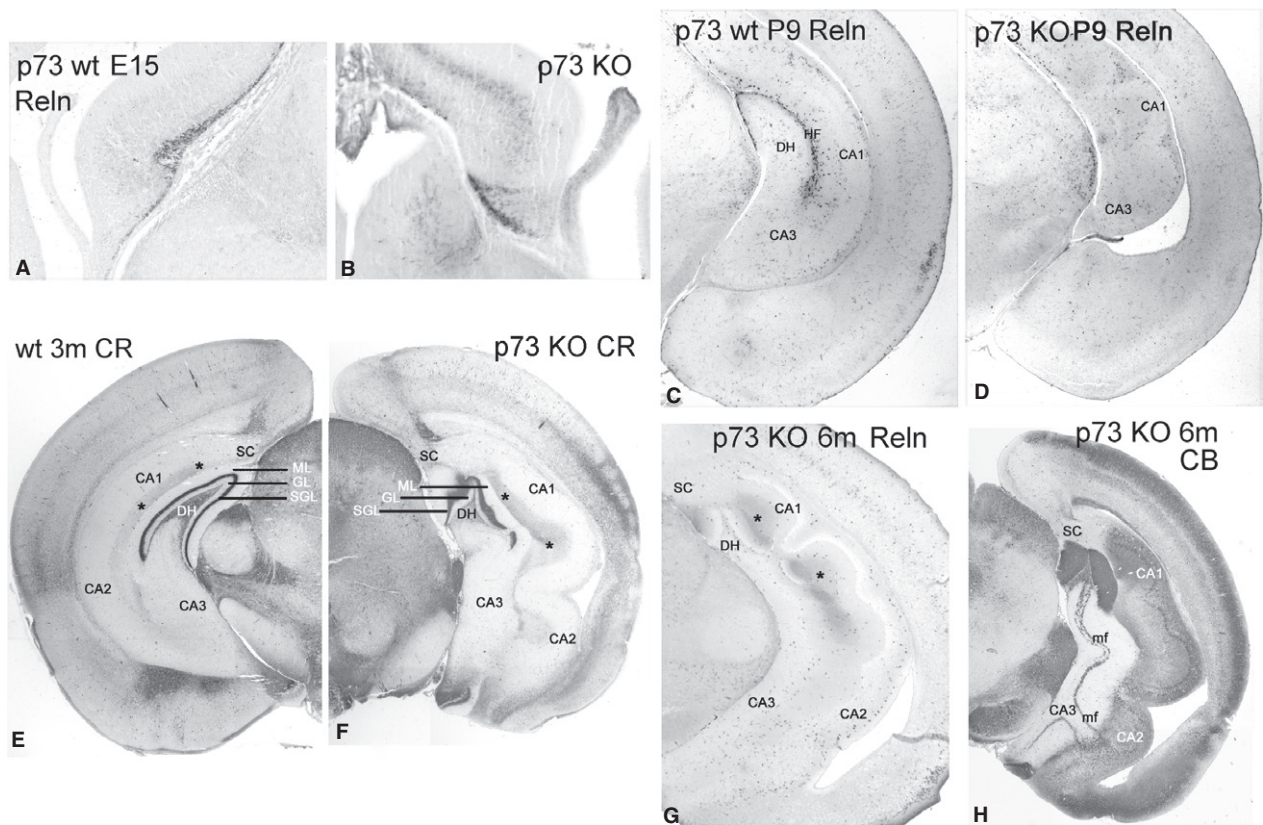
Fig. 8 CRN and the hippocampal fissure in the p73KO mouse. (A,B) Reelin in the wild type (wt) (A) and mutant (B) cortical hem. In the wt, CRN leave the hem and assemble in the HF, which begins to invaginate. In the mutant, Reelin-expression is high in the hem, but CRN do not leave the hem, and the HF fails to invaginate. (C,D) Postnatal HC at 9 days. The HF is densely populated with CRN in the wt (C). In the absence of CRN in the mutant (D), the dentate gyrus (DG) is truncated, and the cornu Ammonis (CA) fields are undulated. (E,F) Calretinin in the adult wt (E) and mutant (F) brain. The truncated and misshaped DG has an intact hilus (DH) whose mossy cells give rise to the intensely immunostained axonal plexus in the supragranular molecular layer (SGL), which seems to invade the subicular complex (SC). (G) Adult mutant brain, Reelin immunostaining. Reelin+ interneurons are irregularly clustered in the stratum lacunosum-moleculare (asterisks), following the folds of CA1. (H) CB-immunostaining of adult mutant HC. The DG is intensely positive and gives rise to the CB+ mossy fibre (mf) tract which innervates CA3. In this case, an aberrant loop extends into CA2. ML, dentate molecular later; GL, dentate granular layer.

The hippocampal fissure of TAp73- and DeltaNp73-deficient mice

As expected from the severe decrease in the number of CRN in TAp73KO embryos (Fig. 7H), the HF of the newborn animals (P1) was abnormal (Fig. 9A,B). This was particularly evident at rostral levels, where the dorsal HF was not invaginated, and where only two or three CRN per section were found (Fig. 9C,D). Reelin+ interneurons were present, but the overall amount of Reelin in the HC was significantly lower (Fig. 9E,F). A defect of the CA fields similar to that of the global p73KO mouse was not evident. However, subiculum and presubiculum lacked a molecular layer, and the infrapyramidal limb of the DG appeared truncated (Fig. 9B). By contrast, at middle levels of the HC, the number of CRN slightly increased, and at the most caudal level there was a considerable population of CRN in the vertical HF (Fig. 10D). However, the caudal-medial wall of the cortex was almost devoid of CRN (Fig. 10D, open arrowheads). The CRN

phenotype of the DNp73KO mice was more difficult to assess. The HF of P2 mice was present at all levels, but appeared shorter compared with the wt, the number of p73/Reelin+ CRN was reduced, and their distribution irregular (Fig. 10A,B). The size and shape of the DG were slightly altered (Fig. 10A). In the caudal HC, the HF was significantly shorter than in the wt (Fig. 10 C,E), and there might be a subtle hippocampal pattern defect (Fig. 10E), as also suggested by Griveau et al. (2010) in the neocortex. In contrast to the TAp73 mutant, the caudal medial wall was well equipped with numerous CRN (Fig. 10E). Unfortunately, we did not have older animals to follow up the outcome of the developmental phenotypes described here. It is clear, though, that neither of the two isoform-deficient mutants came close to the severity of the global p73KO mouse. Only the complete removal of p73 function prevents formation of the HF, suggesting that both isoforms are needed and must closely cooperate. While both p73 isoforms are involved in the formation of HF and HC, no single isoform
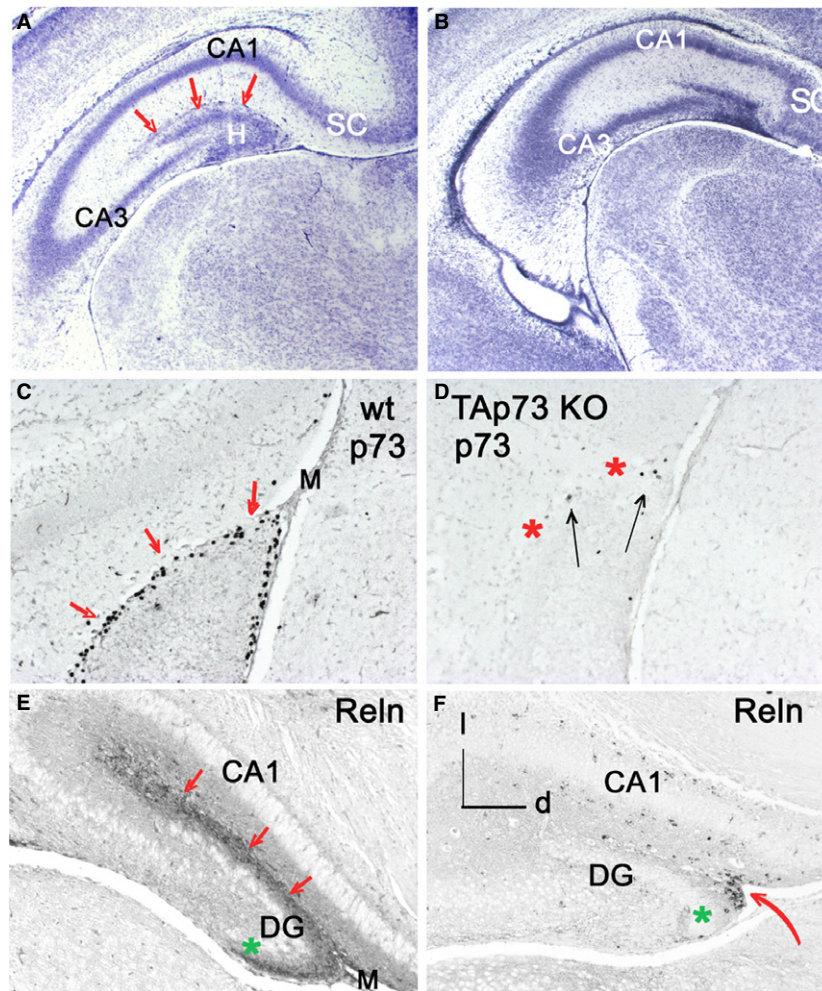
Fig. 9 The dorsal HC in the neonatal (P1) TAp73KO mouse. (A,B) wt (A) and TAp73KO (B) dorsal HC, Nissl staining. In (B), the subicular complex (SC) has an abnormal shape and lacks a molecular layer. The hippocampal fissure, marked in (A) with red arrows, is missing in the mutant. The infrapyramidal blade of the DG is not developing normally. (C) Dorsal HF in wt P1 with numerous p73+ CRN surrounding the DG and populating the HF (red arrows). (D) TAp73KO, P1. The HF is almost absent (red asterisks indicate the missing HF), with only few CRN (arrows) in the rudimentary superficial HF. A strand of meningeal tissue (M) connects with the dorsal tip of the DG in the wt (C), but is missing in the mutant (D). (E) Reelin in CRN in wt P1 dorsal HF (red arrows). In the mutant (F), CRN are present only in a small cluster where the HF rudiment is invaginated (red arrow). Note the overall reduction of Reelin expression due to the almost complete absence of CRN in the mutant HF. Reelin+ interneurons are prominent in CA1. The dentate infrapyramidal limb is truncated in the mutant compared with the wt (green asterisks in E and F). The orientation of sections in (E and F) is indicated in (F): d = dorsal, l = lateral.

was essential, suggesting a partial, albeit not complete functional redundancy. Possibly, a tightly regulated balance in the expression of both isoforms in CRN determines the developmental outcome, i.e. a complete population of CRN in a well-established HF.

Discussion

Development of dorsal HC and indusium griseum

The human dorsal HC is often described as a hippocampal rudiment and is considered a regression of a previously established structure to a simpler or even atrophic

remnant, the IG (Macchi, 1951; Stephan, 1975; Kier et al. 1997; Berger & Alvarez, 1996). The supposed involution of the dorsal HC by 14 GW has been related to the appearance of the CC which appears around 13 GW within a distinct anatomical region at the level of the septum, termed the commissural plate (Rakic & Yakovlev, 1968), and progresses from rostral to caudal. The development of the CC is a complex process that involves early born pioneer neurons in the cingulate cortex (Koester & O'Leary, 1994), as well as specific glial and neuronal guidepost populations (see review by Edwards et al. 2014). We show here that before the emergence of the CC, the dorsal HC has the principal cell compartments also found in the ventral HC at
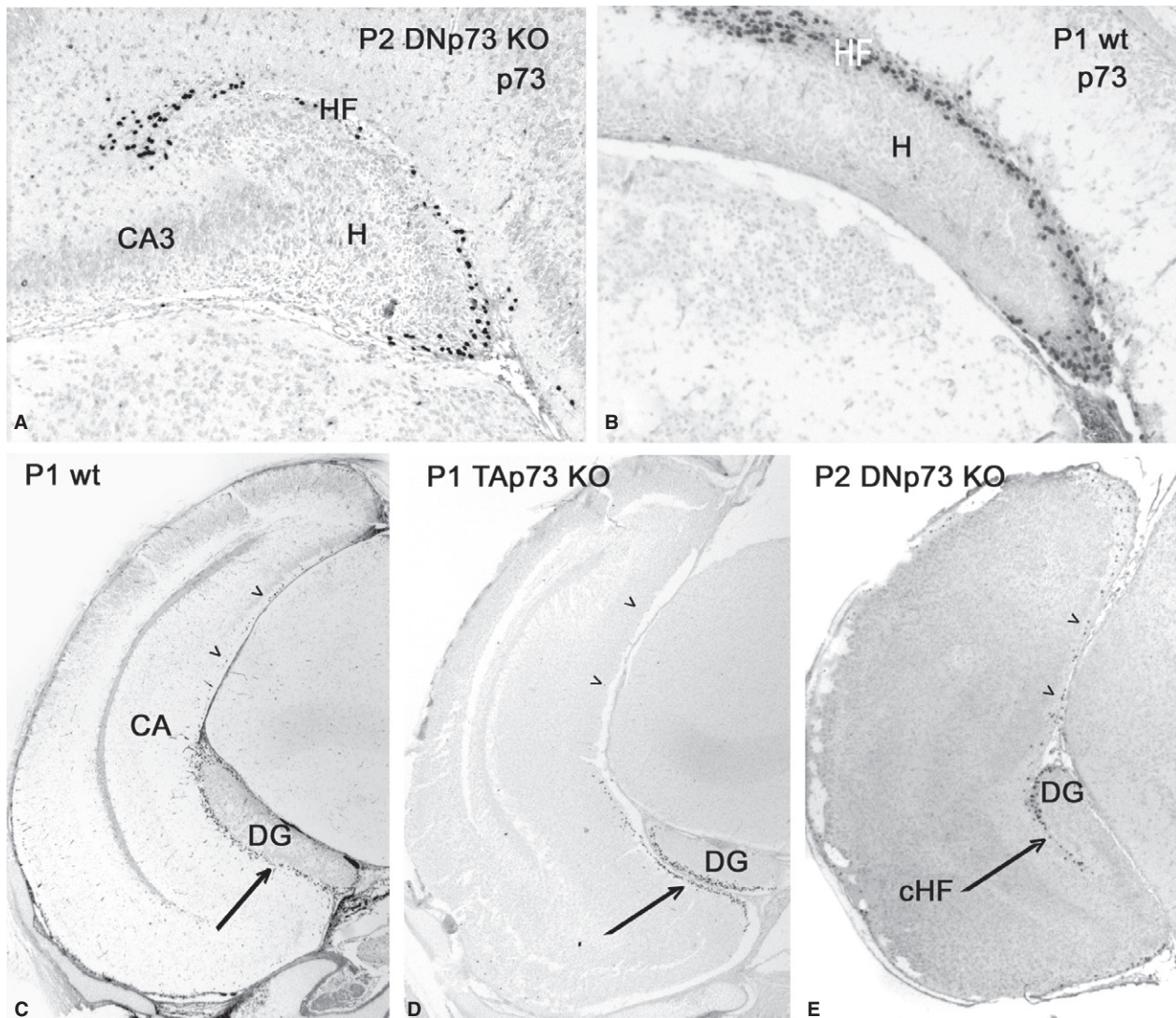
Fig. 10 Hippocampal fissure and CRN in the two p73 mutant mice. (A) Dorsal HC of the DeltaNp73KO mouse at P2. p73+ CRN are less numerous and are irregularly distributed along the HF, which appears shortened. Compare with (B): wt, P1, at approximately the same rostro-caudal level. H, hilus. (C) The caudal HC and HF in P1 wt. p73+ CRN are numerous along the vertical caudal HF (arrow) and in the medial cortical MZ (open arrowheads). The tissue defects in (B–E) are due to the aggressive retrieval treatment of p73 immunohistochemistry. (D) The arrow points to the caudal HF in the P1 TAp73KO mutant. In contrast to the dorsal HC where CRN are almost absent and the HF fails to fold, the ventral HF is present and displays a number of CRN. CRN are absent from the medial cortical wall (open arrowheads). In the DeltaNp73KO mutant (E), the caudal HC appears reduced in size and the HF (arrow) is shortened. CRN are present in the medial cortical MZ (open arrowheads).

this stage. These comprise a radially arranged Ammonic plate containing pyramidal cells and a dentate primordium that develops into a secondary matrix of Prox1+ granule progenitor cells migrating from the primary matrix in the dorsal hippocampal neuroepithelium to the pial surface. A tertiary matrix with a central core of vimentin+ astrocytes, a trail of proliferative cells and a subpial condensed layer of CR+ granule cells suggests further differentiation even after the appearance of the CC. The dorsal HF appears as a shallow groove in the expanded MZ of the Ammonic plate where it meets the dentate anlage. CRN are less numerous in the dorsal HF than in the adjacent callosal sulcus or in

the ventral HC. We attribute this relative paucity to the possibility that most CRN from the dorsal hem migrate into the neocortical MZ and spread over the entire neocortex (Meyer et al. 2002; Yoshida et al. 2006) rather than staying in the rudimentary HF of the IG. This situation is quite different from the development of the mouse dorsal HF where the first event is an indentation of the pial surface concurrent with a collection of CRN (Soriano et al. 1994). However, in mouse, as in many mammalian nonprimate species, the dorsal HC develops and persists despite the appearance of the CC (Strange et al. 2014), suggesting that there is no causal relationship between CC formation and a

supposed regression of the dorsal HC (Macchi, 1951; Stephan, 1975).

We thus propose a transformation of the human dorsal HC into a supracallosal HC or IG, which comprises a laminar refinement and differentiation of its constituents, including a change in orientation from vertical to horizontal, leaving open a possible involution later in life. The fate of the IG is controversial. Tubbs et al. (2013) did not find evidence for neuronal components and described a hypocellular glial tissue between the CC and pia. Laplante et al. (2013) found structural similarities with the DG. The most detailed architectonic account of the human IG is that of Von Economo & Koskinas (1925). Their Area Indusei LB2 is a tongue-shaped, loose assembly of neurons that shows significant variations between individuals. Further studies may solve the question of its fate and functionality. We did not identify in our material the longitudinal fibre tracts (Lancisi nerves) which also take a supracallosal route and whose function is still unknown (Stephan, 1975; Duvernoy, 1998). These tracts may appear later in development.

Cajal-Retzius cells and the hem system

The concept of the cortical hem as a signalling centre adjacent to the choroid plexus (ChP) and rich in *Wnt* genes (*Wnt2b, Wnt3a* and *Wnt5a*) was introduced by Grove et al. (1998). *Wnt* genes in the cortical hem are upregulated when the ChP begins to form, suggesting inductive interactions between the two structures (Grove et al. 1998). Several genes (*Msx2, Wnt5a* and *Bmp7*) are expressed in both cortical hem and ChP epithelium. *Bmp* signalling is essential for the patterning of the telencephalic dorsal midline or roof plate (Furuta et al. 1997; Hebert et al. 2002; Currle et al. 2005; Cheng et al. 2006).

The cortical hem is also the main birthplace of CRN, which are the principal source of Reelin and essential for cortex and HC development (Meyer, 2010). According to Imayoshi et al. (2008), CRN are the first derivatives of the telencephalic midline, which expresses both the proneural bHLH gene *neurogenin 2* (*Ngn2*) and the repressor genes *Hes1* and *Hes5*, and gives rise to two cell lineages, CRN and ChP epithelial cells. *Hes* and *Ngn2* genes antagonistically regulate the specification of non-neural (ChP) vs. neural (CRN) fate.

Studies in lizards, mice and human showed that CRN arise from multiple areas at the interface of the telencephalon and the ChP, including the thalamic eminence at the diencephalic/ChP border, and migrate into neighbouring pallial and subpallial regions (Meyer et al. 2002; Bielle et al. 2005; Cabrera-Socorro et al. 2006; Tissir et al. 2009; Meyer, 2010). Altogether, the CRN origins form the 'hem system' (Meyer, 2010) or 'forebrain hem system', (Roy et al. 2014), the centre of which is the ChP. The transcription factor Lhx2 restricts the extension of the hem system. In the Lhx2-deficient mouse, the various components of the hem system,

including the ChP and thalamic eminence, are greatly expanded at the expense of the adjacent tissues (Roy et al. 2014). CRN, the cortical hem and the telencephalic ChP may thus evolve in concert, coupling surface expansion of the cortex with the expansion of the lateral ventricle (Meyer, 2010).

For a long time, the importance of the ChP in cortical development has been underestimated. The choroid plexus is active in secretion of the cerebrospinal fluid (CSF) and in barrier functions early in corticogenesis (Castañeyra-Ruiz et al. 2016). The secretion of signalling molecules from the ChP into the CSF can regulate the behaviour of neural stem cells, which are in direct contact with the CSF. The ChP modulates neurogenesis and brain development by providing growth- and survival-promoting cues via the CSF (Lehtinen et al. 2013; Johansson, 2014). A transcriptome analysis of the telencephalic vs. hindbrain choroid plexuses in rodent and primate brains (Lun et al. 2015) revealed a regional heterogeneity of gene expression that may contribute to differential region-specific protein secretion into the CSF, and couple the choroid plexuses to the production of signal gradients across the ventricular system. The intense vascularization of the choroid plexuses may provide complementary patterning cues from the anterior vs. posterior circulation (Lun et al. 2015). The anatomical closeness between the ChP epithelium and the developing hippocampal neuroepithelium observed in our material, may thus reflect functional interactions between both structures. In addition, CRN and ChP are the only sites of high expression of p73 in the developing brain (Cabrera-Socorro et al. 2006).

It may be questioned whether human and mouse choroid plexuses are directly comparable. The human telencephalic ChP is not homogeneous: In the atrium of the lateral ventricle, it attains its most caudal position in an enlargement termed the glomus choroideus, and then continues downward into the temporal horn, ending just caudal to the hippocampal head (Duvernoy, 1998). At the hem stage, the future glomus choroideus is directly positioned between dorsal and ventral hem, representing a site of highest potential interactions between the hem system and the ChP. We have termed this junction 'the caudal hem', which constitutes an important source of CRN. In fact, the caudomedial telencephalon, described as being the main origin of cortical CRN (Takiguchi-Hayashi et al. 2004), probably corresponds to our caudal hem. The cortical hem is an organizer of hippocampal development (Tole & Grove, 2001; Bulchand et al. 2001; Subramanian & Tole, 2009). In human fetuses, the dorsal hem may pattern the supracallosal HC, while the caudal hem may act as an organizer of the junction of dorsal and ventral HC, which is located just caudal to the glomus choroideus. In turn, the ventral hem may regulate the patterning of the temporal HC, also giving rise to the first CRN of the HC (Abraham et al. 2004). These anatomical relationships suggest that the hippocampal

formation may be regulated by different organizing centres along its longitudinal axis. There is in fact ample evidence for functional and molecular subdivisions following longitudinal gradients of the human and mouse HC. Three distinct subdivisions (dorsal, intermediate and ventral) were described in the mouse HC based on gene expression, connectivity and function (Fanselow & Dong, 2010; O'Reilly et al. 2015), even though there are differences in gene regulation between mouse and human HC (Hawrylycz et al. 2012; Alzu'bi et al. 2017). Interestingly, in the fetal human HC, a distinct combinatorial expression pattern of transcription factors characterizes dorsal HC (expressing SP8/COUP-TFI) and ventral HC (expressing COUP-TFII/COUP-TFI) (Alzu'bi et al. 2017). In rodents, the posterior/dorsal HC was associated with cognitive functions such as spatial memory (Moser et al. 1995), whereas the ventral HC, closer to the amygdala, has been suggested to be involved in anxiety-based behaviours (Weeden et al. 2015). Strange et al. (2014) proposed a more complex model in which functional long-axis gradients are superimposed on discrete functional domains. Our anatomical definition of the hem system and the various putative signalling centres involved, may provide a better understanding of the longitudinal suborganization of the human HC.

The ventral hippocampal fissure

The HF of the mature HC is a virtual fissure because the molecular layers of CA1 and DG are fused, allowing the fibres of the perforant path to pass through the fissure and reach the DG (Ramón y Cajal, 1911). The early fetal development of the human ventral HC has been studied previously (Abraham et al. 2004) and the following refers to that work, which is confirmed and expanded by our present data. The first event around 11/12 GW is the appearance of a slight inward curve in the hippocampal region containing numerous CRN from the ventral hem. At this stage, the Ammonic and subiculum plates begin to express layer-specific markers CTIP2, SARB2 and CUX1 (Cipriani et al., 2016), and the secondary dentate matrix appears next to the dentate VZ (Cipriani et al. 2017). Between 13 and 16 GW, the HF is wide open, giving rise to the large, triangular 'diffuse zone' in the MZ overlying the Ammonic plate at its border with the dentate anlage (Humphrey, 1967; Berger & Alvarez, 1996). The diffuse zone is filled with p73/Reelin[+] CRN in its outer part, and its inner part also contains many Reelin[+] and GAD[+] interneurons. This stage corresponds to the secondary dentate matrix, when the pial surface of the dentate anlage is almost CRN-free (Abraham et al. 2004). Only after the establishment of the tertiary matrix with the condensation of a recognizable granule cell layer at 16/17 GW does the DG develop a cell-poor molecular layer, which is progressively invaded by late-appearing CRN. These p73/Reelin[+] CRN arrive in the DG via a migratory stream that arises from the ventricular zone near the dentate

notch, and courses along the dentate-fimbrial boundary (Abraham et al. 2004). After the appearance of CRN in the molecular layer of the suprapyramidal blade of the DG around 17 GW, the pial surfaces of the dentate and Ammonic molecular layers fuse, and the HF develops a compact part (Humphrey, 1967) that deepens as the HC continues growing. The formation of the fused HF is thus closely related to the presence of CRN in the molecular layer of the DG, which follows a gradient from the suprapyramidal blade to the later-maturing infrapyramidal blade (Abraham et al. 2004). This reflects the developmental difference between the suprapyramidal blade which develops earlier and the infrapyramidal blade (Arnold & Trojanowski, 1996; Cipriani et al. 2017).

The developing hippocampal fissure and the meninges

The period of the open HF coincides with a massive entrance of blood vessels that profusely ramify in the diffuse zone. The concurrent accumulation of meningeal tissue within the open HF is specific for this stage, and no longer so pronounced after the HF closes. The meninges may exert a mechanical force in opening and deepening the HF, but in addition they may interact with the brain and with CRN in particular through a number of molecular interactions. Increasing evidence points to the meninges as important players in brain development (reviewed by Siegenthaler & Pleasure, 2011). The meninges organize and maintain the pial basement membrane, which provides an attachment site for the radial glial cell endfeet. Destruction of the basement membrane leads to impaired migration along with overmigration out of the brain, and abnormal positioning or even loss of CRN (Halfter et al. 2002). Zic proteins of the zinc-finger transcription factor family are abundantly expressed in both CRN and meninges, and Zic2 mutant mice display a disrupted basement membrane, mislocalized CRN, and a cortical lamination defect resembling type II lissencephaly (Inoue et al. 2008).

The meninges also provide positional cues through the secretion of the chemokine CXCL12 (aka SDF1), which acts as a chemoattractant on its receptor CXCR4 in migrating CRN (Borrell & Marín, 2006), regulating and maintaining their subpial position (Paredes et al. 2006), and determining their functional activity (Marchionni et al. 2010). CXCR4 is, however, also present in cortical interneurons (Stumm et al. 2003; Fan et al. 2018). Even though we detected expression of CXCR4 in CRN of the neocortex (Meyer & González-Gómez, 2018a,b), high background staining, perhaps due to the high density of CXCR4^{+} interneurons, prevented us from identifying immunostained CRN in the HC.

Furthermore, the meninges produce the diffusible lipophilic molecule retinoic acid, which is a strong induction and differentiation signal in early brain development and forebrain morphogenesis (Ribes et al. 2006; Siegenthaler

et al. 2009). All-*trans* retinoic acid (atRA) is synthetized in the leptomeninges at the time of forebrain patterning (Siegenthaler et al. 2009). The meninges also express the cytoplasmic binding and transporter proteins CRABP I and CRABP II (cellular RA binding proteins type I and II), which may convey atRA to the endfeet of radial glia (Ruberte et al. 1993). Interestingly, CRN at midgestation express CRABPII RNA (Fan et al. 2018), suggesting a role of CRN in atRA signalling. These examples show that meningeal signalling, usually neglected, is critically involved in brain development. Even the meninges-associated vasculature is crucial for regulating brain blood flow, CSF production and maintenance of the neuronal integrity of the cerebral hemispheres via expression of genes of the retinoic acid and lipid processing categories (Bowyer et al. 2013).

The hippocampal fissure and p73 expression in CRN

The HF initially forms as an open groove whose pial surface is populated by CRN and contacted by the endfeet of radial glia in the Ammonic and dentate plates (Eckenhoff & Rakic, 1984; Abraham et al. 2004). However, the HF folds and deepens, and gradually transforms into a fused, virtual fissure. The continued presence of blood vessels surrounded by meningeal tissue in the Virchow-Robin spaces within the fused HF is a reminder of the early invasion of meninges described above. In rodents, the basic steps of HC development are the same as in human (Altman & Bayer, 1990a,b), even though the mesenchymal component of fissure formation is less evident. In mice, dentate progenitor cells assemble in a transient subpial neurogenetic niche within the HF before they relocate to the subgranular layer, the site of persisting neurogenesis (Li et al. 2009). In addition, the subpial niche gives rise to a specific type of glia that is arranged parallel to the HF and contributes to the separation of the molecular layers of CA and DG (Sievers et al. 1992; Brunne et al. 2010).

The formation of the HF is thus a complex multifactorial process influenced by neuronal, glial and meningeal interactions. The transcriptome of CRN (Fan et al. 2018; Iacono et al. 2018) includes a number of important transcription factors and morphogens, mutations of which may negatively impact on the morphogenesis of the HF. There are many mouse mutants defective in genes variously expressed in the cortical hem, dentate gyrus, CRN or specific hippocampal glia bundles that show an abnormal HF (Zhao et al. 2006; Barry et al. 2008; Hodge et al. 2013). The protein p73 is essential for the development of CRN and the formation of the HF (Meyer et al. 2004). We show here that CRN are born in the p73-deficient hem, but are unable to leave their birthplace and die. The p73-deficient hem itself does not appear abnormal in size and shape, and we observed normal expression of Wnt3a (data not published). The absence of CRN is surprisingly well tolerated by the developing cortex (Medina-Bolívar et al.

2014). The most striking malformation of the p73KO mouse is the hippocampal dysgenesis, which we attribute to the loss of CRN and subsequent lack of HF formation. Already at E12, CRN fail to aggregate within the shallow curve that marks the early HF, whereas in wt embryos the HF deepens and becomes densely populated by CRN. As p73KO mice can live for several years (Talos et al. 2010; Medina-Bolívar et al. 2014), it is possible to assess the long-term consequences of the absence of an HF on HC morphology. In the adult mutant, the border between the dentate molecular layer, distinctly visualized with CB immunostaining, and the stratum lacunosum-moleculare of CA1 is sharp and well delineated, indicating that there is no invasion of dentate tissue into Ammonic territory, and vice versa. Explant experiments early in HC development demonstrated that hippocampal CA fields develop autonomously, even in the absence of a cortical hem (Tole et al. 1997; Tole & Grove, 2001). By contrast, the HF is not intrinsic to HC formation but requires the presence of CRN. Because the HF in *reeler* mice develops normally (Lambert de Rouvroit & Goffinet, 1998), we conclude that the absence of the HF is not due to a loss of Reelin in CRN, but rather to a loss of p73 in CRN. Reelin[+] interneurons, which are abundant, although malpositioned, in the stratum lacunosum-moleculare, are not able to compensate for the loss of CRN. The undulations of the CA fields suggest that the HF acts as a central axis that maintains the separation between CA1/2 and CA3. In its absence, CA1/2 and CA3 seem to fuse in some places and form ring-like structures, particularly at an intermediate level where dorsal and ventral HC merge. This malformation appears around birth and is not the consequence of a severe hydrocephaly that might compress CA1 and CA2.

The dentate malformation, characterized as an absence of the infrapyramidal blade (Yang et al. 2000), may also be attributed to the loss of the HF. The integrity of the secondary glial scaffold (Hartmann et al. 1992; Sievers et al. 1992) is necessary for the normal development of the neurogenic niche in the HF and the development of the infrapyramidal blade. Chemical ablation of the midline meninges produces loss or malposition of the infrapyramidal blade, which closely resembles the adult dentate phenotype of the p73 mutant: the infrapyramidal limb is truncated and directed dorsally. Compensatory mechanisms later in life may correct an initial lack of the infrapyramidal blade and give rise to an aberrant one (Hartmann et al. 1992).

The question is whether the severe malformations of CA and DG are compatible with a functional HC. Mutant p73 perform poorly in multiple cognitive tests designed to assess memory, learning and sensory motor ability (Talos et al. 2010; Medina-Bolívar et al. 2014), in keeping with our experience that the animals were unable to participate in conditioned reflex tests such as the shuttle box. Memory and learning are thus profoundly impaired.

We provide here an anatomical description of the hippocampal phenotype of the p73KO mouse, which, combined with our analysis of human HC development, suggests that the loss of p73 leads to the loss of the HF, possibly through an interaction between CRN and the meninges/meningeal vessels. What could be the underlying molecular mechanisms that may take place in CRN and give rise to the striking abnormalities of the CA fields? The p73 protein may regulate the expression of a multitude of transcription factors, receptors and morphogens present in the transcriptome of CRN (Fan et al. 2018; Iacono et al. 2018). Regulation of p73 and its downstream targets in the brain remains largely unexplored *in vivo*.

TAp73 versus DeltaNp73

To shed light on the question of which N-terminal isoform is important for hippocampal development, we examined embryonic and early postnatal brains of isoform-specific mutant mice deficient in either TAp73 (Tomasini et al. 2008) or DeltaNp73 (Tissir et al. 2009). TAp73 is the transactivation-competent isoform and DeltaNp73 is the dominant- negative isoform. They have opposing pro- and anti-apoptotic roles, respectively (Grob et al. 2001; Pozniak et al. 2002; Jacobs et al. 2006; Ramadan et al. 2005). The p73 protein is dispensable for commitment to neural stem cell fate but is essential for neural stem cell maintenance and for blocking premature differentiation (Alexandrova et al. 2013). Metabolic pathways are also transcriptionally regulated by p73. Loss of TAp73 or DeltaNp73 triggers selective biochemical changes in glycolysis, membrane phospholipids and metabolism of neurotransmitters. Specifically, loss of TAp73 seems to increase glycolysis, whereas loss of DeltaNp73 reduces glucose metabolism (Agostini et al. 2018). TAp73 also regulates the synthesis of the enzyme glutaminase isoform 2 (GLS2) that converts glutamine into glutamate. TAp73 loss affects GABA and glutamate levels in cortical neurons, and the regulation of neurotransmitters may be one of the mechanisms that mediate the effects of p73 on neurons (Velletri et al. 2013).

We found that both mutants had lower numbers of p73+ CRN during embryonic life, with a more significant decrease in the TAp73KO. At birth, the TAp73KO mouse has the more severe brain phenotype, displaying some of the features of the global p73KO, such as the folding defect of the dorsal HF accompanied by a near absence of CRN in the medial cortex, arrest in the development of the dentate infrapyramidal blade, and loss of the MZ in the subicular complex. A truncated or missing infrapyramidal dentate blade was reported in 4-month-old mutants (Tomasini et al. 2008), although the CA fields apparently do not show the severe malformation of the global p73KO. By contrast, the DeltaNp73 mutant had more subtle deficits, which were difficult to interpret. In addition to a reduced number of CRN

(Tissir et al. 2009), the postnatal HC appeared differently patterned, with a shortened HF and a reduced DG size. Changes in cortical regionalization of the DeltaNp73 mutant have been reported by Griveau et al. (2010).

Importantly, even when all the defects from both isoform-specific mutants are considered together, this does not add up to the severity of the global p73KO, and it is difficult to explain how the complete loss of p73 can have such a dramatic effect on CRN. A precisely balanced coexpression and functional synergy of both isoforms may be required for a normal development of CRN.

Conflict of interest

The corresponding author, on behalf of the coauthors, declares no conflict of interest.

Author contributions

G.M. and E.G.A. conceived the experiments. U.M., A.N. and F.T. provided the TAp73 and DeltaNp73 mutant mice, respectively. G.M., E.G.A. and M.G.G. performed the experiments, analysed the data and wrote the manuscript. All authors approved the manuscript.

Ethical approval

All applicable international, national and institutional guidelines for the care and use of animals were followed.

References

Abraham H, Meyer G (2003) Reelin-expressing neurons in the postnatal and adult human hippocampal formation. *Hippocampus* **13**, 715–727.

Abraham H, Pérez-García CG, Meyer G (2004) p73 and Reelin in Cajal-Retzius cells of the developing human hippocampal formation. *Cereb Cortex* **14**, 484–495.

Abrahám H, Veszprémi B, Kravják A, et al. (2009) Ontogeny of calbindin immunoreactivity in the human hippocampal formation with a special emphasis on granule cells of the dentate gyrus. *Int J Dev Neurosci* **27**, 115–127.

Agostini M, Niklison-Chirou MV, Annicchiarico-Petruzzelli MM, et al. (2018) p73 regulates primary cortical neuron metabolism: a global metabolic profile. *Mol Neurobiol* **55**, 3237–3250.

Alexandrova EM, Talos F, Moll UM (2013) p73 is dispensable for commitment to neural stem cell fate, but is essential for neural stem cell maintenance and for blocking premature differentiation. *Cell Death Differ* **20**, 368.

Altman J, Bayer SA (1990a) Migration and distribution of two populations of hippocampal granule cell precursors during

the perinatal and postnatal periods. *J Comp Neurol* **301**, 365–381.

Altman J, Bayer SA (1990b) Mosaic organization of the hippocampal neuroepithelium and the multiple germinal sources of dentate granule cells. *J Comp Neurol* **301**, 325–342.

Alzu'bi A, Lindsay SJ, Harkin LF, et al. (2017) The transcription factors COUP-TFI and COUP-TFII have distinct roles in arealisation and GABAergic interneuron specification in the early human fetal telencephalon. *Cereb Cortex* **27**, 4971–4987. https://doi.org/10.1093/cercor/bhx185.

Arnold SE, Trojanowski JQ (1996) Human fetal hippocampal development: I. Cytoarchitecture, myeloarchitecture, and neuronal morphologic features. *J Comp Neurol* **367**, 274–292.

Barry G, Piper M, Lindwall C, et al. (2008) Specific glial populations regulate hippocampal morphogenesis. *J Neurosci* **28**, 12328–12340. https://doi.org/0.1523/jneurosci.4000-08.2008.

Bayer S, Altman J (2005) *Atlas of Human Central Nervous System Development.* Boca Raton: CRC Press.

Berger B, Alvarez C (1996) Neurochemical development of the hippocampal region in the fetal rhesus monkey, III: calbindin-D28K, calretinin and parvalbumin with special mention of cajal-retzius cells and the retrosplenial cortex. *J Comp Neurol* **366**, 674–699.

Bielle F, Griveau A, Narboux-Neme N, et al. (2005) Multiple origins of Cajal-Retzius cells at the borders of the developing pallium. *Nat Neurosci* **8**, 1002–1012.

Borrell V, Marín O (2006) Meninges control tangential migration of hem-derived Cajal-Retzius cells via CXCL12/CXCR4 signaling. *Nat Neurosci* **9**, 1284–1293.

Bowyer JF, Patterson TA, Saini UT, et al. (2013) Comparison of the global gene expression of choroid plexus and meninges and associated vasculature under control conditions and after pronounced hyperthermia or amphetamine toxicity. *BMC Genom* **14**, 147.

Brandt MD, Jessberger S, Steiner B, et al. (2003) Transient calretinin expression defines early postmitotic step of neuronal differentiation in adult hippocampal neurogenesis of mice. *Mol Cell Neurosci* **24**, 603–613.

Brunne B, Zhao S, Derouiche A, et al. (2010) Origin, maturation, and astroglial transformation of secondary radial glial cells in the developing dentate gyrus. *Glia* **58**, 1553–1569. https://doi.org/10.1002/glia.21029.

Bulchand S, Grove EA, Porter FD, et al. (2001) LIM-homeodomain gene Lhx2 regulates the formation of the cortical hem. *Mech Dev* **100**, 165–175.

Cabrera-Socorro A, Pueyo-Morlans M, Suarez-Sola ML, et al. (2006) Multiple isoforms of the tumor protein p73 are expressed in the adult human telencephalon and choroid plexus and present in the cerebrospinal fluid. *Eur J Neurosci* **23**, 2109–2118.

Castañeyra-Ruiz L, González-Marrero I, Hernández-Abad LG, et al. (2016) A distal to proximal gradient of human choroid plexus development, with antagonistic expression of Glut1 and AQP1 in mature cells vs. calbindin and PCNA in proliferative cells. *Front Neuroanat* **10**, 87.

Cheng X, Hsu CM, Currle DS, et al. (2006) Central roles of the roof plate in telencephalic development and holoprosencephaly. *J Neurosci* **26**, 7640–7649.

Cipriani S, Nardelli J, Verney C, et al. (2016) Dynamic expression patterns of progenitor and pyramidal neuron layer markers in the developing human hippocampus. *Cereb Cortex* **26**, 1255–1271. https://doi.org/10.1093/cercor/bhv079.

Cipriani S, Journiac N, Nardelli J, et al. (2017) Expression patterns of progenitor and neuron layer markers in the developing human dentate gyrus and fimbria. *Cereb Cortex* **27**, 358–372.

Currle DS, Cheng X, Hsu CM, et al. (2005) Direct and indirect roles of CNS dorsal midline cells in choroid plexus epithelia formation. *Development* **132**, 3549–3559.

D'Arcangelo G, Miao GG, Chen SC, et al. (1995) A protein related to extracellular matrix proteins deleted in the mouse mutant reeler. *Nature* **374**, 719–723.

Del Río JA, Martínez A, Fonseca M, et al. (1995) Glutamate-like immunoreactivity and fate of Cajal-Retzius cells in the murine cortex as identified with calretinin antibody. *Cereb Cortex* **5**, 13–21.

Del Río JA, Heimrich B, Supèr H, et al. (1996) Differential survival of Cajal-Retzius cells in organotypic cultures of hippocampus and neocortex. *J Neurosci* **16**, 6896–6907.

Del Río JA, Heimrich B, Borrell V, et al. (1997) A role for Cajal-Retzius cells and reelin in the development of hippocampal connections. *Nature* **385**, 70–74.

Drakew A, Frotscher M, Deller T, et al. (1998) Developmental distribution of a reeler gene-related antigen in the rat hippocampal formation visualized by CR-50 immunocytochemistry. *Neuroscience* **82**, 1079–1086.

Duvernoy HM (1998) *The Human Hippocampus.* Vienna: Springer.

Eckenhoff MF, Rakic P (1984) Radial organization of the hippocampal dentate gyrus: a Golgi, ultrastructural, and immunocytochemical analysis in the developing rhesus monkey. *J Comp Neurol* **223**, 1–21.

Edwards TJ, Sherr EH, Barkovich AJ, et al. (2014) Clinical, genetic and imaging findings identify new causes for corpus callosum development syndromes. *Brain* **137**, 1579–1613.

Fan X, Dong J, Zhong S, et al. (2018) Spatial transcriptomic survey of human embryonic cerebral cortex by single-cell RNA-seq analysis. *Cell Res* **28**, 730–745.

Fanselow MS, Dong HW (2010) Are the dorsal and ventral hippocampus functionally distinct structures? *Neuron* **65**, 7–19.

Frotscher M (1998) Cajal-Retzius cells, reelin, and the formation of layers. *Curr Opin Neurobiol* **8**, 570–575.

Furuta Y, Piston DW, Hogan BL (1997) Bone morphogenetic proteins (BMPs) as regulators of dorsal forebrain development. *Development* **124**, 2203–2212.

Gonzalez-Cano L, Herreros-Villanueva M, Fernandez-Alonso R, et al. (2010) p73 deficiency results in impaired self renewal and premature neuronal differentiation of mouse neural progenitors independently of p53. *Cell Death Dis* **1**, e109.

González-Gómez M, Meyer G (2014) Dynamic expression of calretinin in embryonic and early fetal human cortex. *Front Neuroanat* **8**, 41.

Griveau A, Borello U, Causeret F, et al. (2010) A novel role for Dbx1-derived Cajal-Retzius cells in early regionalization of the cerebral cortical neuroepithelium. *PLoS Biol* **8**, e1000440.

Grob TJ, Novak U, Maisse C, et al. (2001) Human delta Np73 regulates a dominant negative feedback loop for TAp73 and p53. *Cell Death Differ* **8**, 1213–1223.

Grove EA, Tole S, Limon J, et al. (1998) The hem of the embryonic cerebral cortex is defined by the expression of multiple Wnt genes and is compromised in Gli3-deficient mice. *Development* **125**, 2315–2325.

Halfter W, Dong S, Yip YP, et al. (2002) A critical function of the pial basement membrane in cortical histogenesis. *J Neurosci* **22**, 6029–6040.

Hartmann D, Sievers J, Pehlemann FW, et al. (1992) Destruction of meningeal cells over the medial cerebral hemisphere of newborn hamsters prevents the formation of the infrapyramidal blade of the dentate gyrus. *J Comp Neurol* **320**, 33–61.

Hawrylycz MJ, Lein ES, Guillozet-Bongaarts AL, et al. (2012) An anatomically comprehensive atlas of the adult human brain transcriptome. *Nature* **489**, 391–399.

Hebert JM, Mishina Y, McConnell SK (2002) BMP signaling is required locally to pattern the dorsal telencephalic midline. *Neuron* **35**, 1029–1041.

Hernández-Acosta NC, Cabrera-Socorro A, Morlans MP, et al. (2011) Dynamic expression of the p53 family members p63 and p73 in the mouse and human telencephalon during development and in adulthood. *Brain Res* **1372**, 29–40.

Hevner RF, Neogi T, Englund C, et al. (2003) Cajal-Retzius cells in the mouse: transcription factors, neurotransmitters, and birthdays suggest a pallial origin. *Brain Res Dev Brain Res* **141**, 39–53.

Hodge RD, Garcia AJ, Elsen GE, et al. (2013) Tbr2 expression in Cajal-Retzius cells and intermediate neuronal progenitors is required for morphogenesis of the dentate gyrus. *J Neurosci* **33**, 4165–4180.

Holembowski L, Kramer D, Riedel D, et al. (2014) TAp73 is essential for germ cell adhesion and maturation in testis. *J Cell Biol* **204**, 1173–1190.

Humphrey T (1967) The development of the human hippocampal fissure. *J Anat* **101**, 655–676.

Iacono G, Mereu E, Guillaumet-Adkins A, et al. (2018) bigSCale: an analytical framework for big-scale single-cell data. *Genome Res* **28**, 878–890.

Imayoshi I, Shimogori T, Ohtsuka T, et al. (2008) Hes genes and neurogenin regulate non-neural versus neural fate specification in the dorsal telencephalic midline. *Development* **135**, 2531–2541.

Inoue T, Ogawa M, Mikoshiba K, et al. (2008) Zic deficiency in the cortical marginal zone and meninges results in cortical lamination defects resembling those in type II lissencephaly. *J Neurosci* **28**, 4712–4725.

Inoue S, Tomasini R, Rufini A, et al. (2014) TAp73 is required for spermatogenesis and the maintenance of male fertility. *Proc Natl Acad Sci USA* **111**, 1843–1848.

Jacobs WB, Kaplan DR, Miller FD (2006) The p53 family in nervous system development and disease. *J Neurochem* **97**, 1571–1584.

Johansson PA (2014) The choroid plexuses and their impact on developmental neurogenesis. *Front Neurosci* **8**, 340.

Kaghad M, Bonnet H, Yang A, et al. (1997) Monoallelically expressed gene related to p53 at 1p36, a region frequently deleted in neuroblastoma and other human cancers. *Cell* **90**, 809–819.

Kier EL, Kim JH, Fulbright RK, et al. (1997) Embryology of the human fetal hippocampus: MR imaging, anatomy, and histology. *AJNR Am J Neuroradiol* **18**, 525–532.

Koester SE, O'Leary DD (1994) Axons of early generated neurons in cingulate cortex pioneer the corpus callosum. *J Neurosci* **4**, 6608–6620.

Lambert de Rouvroit C, Goffinet AM (1998) The reeler mouse as a model of brain development. *Adv Anat Embryol Cell Biol* **150**, 1–106.

Laplante F, Mnie-Filali O, Sullivan RM (2013) A neuroanatomical and neurochemical study of the indusium griseum and anterior hippocampal continuation: comparison with dentate gyrus. *J Chem Neuroanat* **50**, 39–47.

Lehtinen MK, Bjornsson CS, Dymecki SM, et al. (2013) The choroid plexus and cerebrospinal fluid: emerging roles in development, disease, and therapy. *J Neurosci* **33**, 17553–17559.

Li G, Kataoka H, Coughlin SR, et al. (2009) Identification of a transient subpial neurogenic zone in the developing dentate gyrus and its regulation by Cxcl12 and reelin signaling. *Development* **136**, 327–335.

Lun MP, Johnson MB, Broadbelt KG, et al. (2015) Spatially heterogeneous choroid plexus transcriptomes encode positional identity and contribute to regional CSF production. *J Neurosci* **35**, 4903–4916. https://doi.org/10.1523/jneurosci.3081-14.2015.

Macchi G (1951) The ontogenic development of the telencephalon in man. *J Comp Neurol* **95**, 245–305.

Marchionni I, Takács VT, Nunzi MG, et al. (2010) Distinctive properties of CXC chemokine receptor 4-expressing Cajal-Retzius cells versus GABAergic interneurons of the postnatal hippocampus. *J Physiol* **588**, 2859–2878.

Medina-Bolívar C, González-Arnay E, Talos F, et al. (2014) Cortical hypoplasia and ventriculomegaly of p73-deficient mice: developmental and adult analysis. *J Comp Neurol* **522**, 2663–2679.

Meyer G (2010) Building a human cortex: the evolutionary differentiation of Cajal-Retzius cells and the cortical hem. *J Anat* **217**, 334–343.

Meyer G (2011) p73: a complex gene for building a complex brain. *Cell Cycle* **10**, 1188–1189.

Meyer G, Goffinet AM (1998) Prenatal development of reelin immunoreactive neurons in the human neocortex. *J Comp Neurol* **397**, 29–40.

Meyer G, González-Gómez M (2018a) The subpial granular layer and transient versus persisting Cajal-Retzius neurons of the fetal human cortex. *Cereb Cortex* **28**, 2043–2058.

Meyer G, González-Gómez M (2018b) The heterogeneity of human Cajal-Retzius neurons. *Semin Cell Dev Biol* **76**, 101–111.

Meyer G, Schaaps JP, Moreau L, et al. (2000) Embryonic and early fetal development of the human neocortex. *J Neurosci* **20**, 1858–1868.

Meyer G, Perez-Garcia CG, Abraham H, et al. (2002) Expression of p73 and Reelin in the developing human cortex. *J Neurosci* **22**, 4973–4986.

Meyer G, Cabrera-Socorro A, Perez-Garcia CG, et al. (2004) Developmental roles of p73 in Cajal-Retzius cells and cortical patterning. *J Neurosci* **24**, 9878–9887.

Moser MB, Moser EI, Forrest E, et al. (1995) Spatial learning with a minislab in the dorsal hippocampus. *Proc Natl Acad Sci U S A* **92**, 9697–9701.

Nemajerova A, Kramer D, Siller SS, et al. (2016) TAp73 is a central transcriptional regulator of airway multiciliogenesis. *Genes Dev* **30**, 1300–1312.

Niklison-Chirou MV, Killick R, Knight RA, et al. (2016) How does p73 cause neuronal defects? *Mol Neurobiol* **53**, 4509–4520.

Ogawa M, Miyata T, Nakajima K, et al. (1995) The reeler gene associated antigen on Cajal-Retzius neurons is a crucial molecule for laminar organization of cortical neurons. *Neuron* **14**, 899–912.

O'Reilly KC, Flatberg A, Islam S, et al. (2015) Identification of dorsal-ventral hippocampal differentiation in neonatal rats. *Brain Struct Funct* **220**, 2873–2893.

Paredes MF, Li G, Berger O, et al. (2006) Stromal-derived factor-1 (CXCL12) regulates laminar position of Cajal-Retzius cells in normal and dysplastic brains. *J Neurosci* **26**, 9404–9412.

Pozniak CD, Barnabe-Heider F, Rymar VV, et al. (2002) p73 is required for survival and maintenance of CNS neurons. *J Neurosci* **22**, 9800–9809.

Rakic P, Yakovlev PI (1968) Development of the corpus callosum and cavum septi in man. *J Comp Neurol* **132**, 45–72.

Ramadan S, Terrinoni A, Catani MV, et al. (2005) p73 induces apoptosis by different mechanisms. *Biochem Biophys Res Commun* **331**, 713–717.

Ramón y Cajal S (1909–1911) *Histologie du Système Nerveux de L'homme et des Vertébrés*. Paris: Maloine.

Ribes V, Wang Z, Dollé P, et al. (2006) Retinaldehyde dehydrogenase 2 (RALDH2)-mediated retinoic acid synthesis regulates early mouse embryonic forebrain development by controlling FGF and sonic hedgehog signaling. *Development* **133**, 351–361.

Roy A, Gonzalez-Gomez M, Pierani A, et al. (2014) Lhx2 regulates the development of the forebrain hem system. *Cereb Cortex* **24**, 1361–1372. https://doi.org/10.1093/cercor/bhs421.

Ruberte E, Friederich V, Chambon P, et al. (1993) Retinoic acid receptors and cellular retinoid binding proteins. III. Their differential transcript distribution during mouse nervous system development. *Development* **118**, 267–282.

Seress L, Abrahám H, Czéh B, et al. (2008) Calretinin expression in hilar mossy cells of the hippocampal dentate gyrus of non-human primates and humans. *Hippocampus* **18**, 425–434.

Siegenthaler JA, Pleasure SJ (2011) We have got you 'covered': how the meninges control brain development. *Curr Opin Genet Dev* **21**, 249–255.

Siegenthaler JA, Ashique AM, Zarbalis K, et al. (2009) Retinoic acid from the meninges regulates cortical neuron generation. *Cell* **139**, 597–609.

Sievers J, Hartmann D, Pehlemann FW, et al. (1992) Development of astroglial cells in the proliferative matrices, the granule cell layer, and the hippocampal fissure of the hamster dentate gyrus. *J Comp Neurol* **320**, 1–32.

Soriano E, Del Río JA, Martínez A, et al. (1994) Organization of the embryonic and early postnatal murine hippocampus. I. Immunocytochemical characterization of neuronal populations in the subplate and marginal zone. *J Comp Neurol* **342**, 571–595.

Stephan H (1975) Allocortex. In: *Handbuch der Mikroskopischen Anatomie des Menschen* (ed. Bargmann W), Vol. 4, Part 9, pp. 998. Berlin: Springer-Verlag.

Stergiopoulos A, Elkouris M, Politis PK (2015) Prospero-related homeobox 1 (Prox1) at the crossroads of diverse pathways during adult neural fate specification. *Front Cell Neurosci* **8**, 454. https://doi.org/10.3389/fncel.2014.00454.

Strange BA, Witter MP, Lein ES, et al. (2014) Functional organization of the hippocampal longitudinal axis. *Nat Rev Neurosci* **15**, 655–669.

Stumm RK, Zhou C, Ara T, et al. (2003) CXCR4 regulates interneuron migration in the developing neocortex. *J Neurosci* **23**, 5123–5130.

Subramanian L, Tole S (2009) Mechanisms underlying the specification, positional regulation, and function of the cortical hem. *Cereb Cortex* **19**(Suppl 1), i90–i95.

Supèr H, Martínez A, Del Río JA, et al. (1998) Involvement of distinct pioneer neurons in the formation of layer-specific connections in the hippocampus. *J Neurosci* **18**, 4616–4626.

Takiguchi-Hayashi K, Sekiguchi M, Ashigaki S, et al. (2004) Generation of reelin-positive marginal zone cells from the caudomedial wall of telencephalic vesicles. *J Neurosci* **24**, 2286–2295.

Talos F, Abraham A, Vaseva AV, et al. (2010) p73 is an essential regulator of neural stem cell maintenance in embryonal and adult CNS neurogenesis. *Cell Death Differ* **17**, 1816–1829.

Tissir F, Goffinet AM (2003) Reelin and brain development. *Nat Rev Neurosci* **4**, 496–505.

Tissir F, Lambert de Rouvroit C, Goffinet AM (2002) The role of reelin in the development and evolution of the cerebral cortex. *Braz J Med Biol Res* **35**, 1473–1484.

Tissir F, Ravni A, Achouri Y, et al. (2009) DeltaNp73 regulates neuronal survival *in vivo*. *Proc Natl Acad Sci U S A* **106**, 16871–16876.

Tole S, Grove EA (2001) Detailed field pattern is intrinsic to the embryonic mouse hippocampus early in neurogenesis. *J Neurosci* **21**, 1580–1589.

Tole S, Christian C, Grove EA (1997) Early specification and autonomous development of cortical fields in the mouse hippocampus. *Development* **124**, 4959–4970.

Tomasini R, Tsuchihara K, Wilhelm M, et al. (2008) TAp73 knockout shows genomic instability with infertility and tumor suppressor functions. *Genes Dev* **22**, 2677–2691.

Tubbs RS, Prekupec M, Loukas M, et al. (2013) The indusium griseum: anatomic study with potential application to callosotomy. *Neurosurgery* **73**, 312–315.

Velletri T, Romeo F, Tucci P, et al. (2013) GLS2 is transcriptionally regulated by p73 and contributes to neuronal differentiation. *Cell Cycle* **12**, 3564–3573.

Verney C, Derer P (1995) Cajal-Retzius neurons in human cerebral cortex at midgestation show immunoreactivity for neurofilament and calcium-binding proteins. *J Comp Neurol* **359**, 144–153.

Vikhreva P, Melino G, Amelio I (2018) p73 Alternative splicing: exploring a biological role for the c-terminal isoforms. *J Mol Biol* **430**, 1829–1838.

Von Economo C, Koskinas GN (1925) *Die Cytoarchitektonik der Hirnrinde des erwachsenen Menschen*. Berlin: J. Springer.

Weeden CS, Roberts JM, Kamm AM, et al. (2015) The role of the ventral dentate gyrus in anxiety-based behaviors. *Neurobiol Learn Mem* **118**, 143–149.

Yang A, Walker N, Bronson R, et al. (2000) p73-deficient mice have neurological, pheromonal and inflammatory defects but lack spontaneous tumours. *Nature* **404**, 99–103.

Yoshida M, Assimacopoulos S, Jones KR, et al. (2006) Massive loss of Cajal-Retzius cells does not disrupt neocortical layer order. *Development* **133**, 537–545.

Zhao T, Kraemer N, Oldekamp J, et al. (2006) Emx2 in the developing hippocampal fissure region. *Eur J Neurosci* **23**, 2895–28907.